

6-2022

STATIC TESTING OF HYBRID ROCKET ENGINE USING BIOMASS WASTE

Saleh Mohammed Musaed Badi

Follow this and additional works at: https://scholarworks.uaeu.ac.ae/all_theses



Part of the [Aerospace Engineering Commons](#)



MASTER THESIS NO. 2022: 50

College of Engineering

Department of Mechanical and Aerospace Engineering

**STATIC TESTING OF HYBRID ROCKET ENGINE
USING BIOMASS WASTE**

Saleh Mohammed Musaed Badi



June 2022

United Arab Emirates University

College of Engineering

Department of Mechanical and Aerospace Engineering

STATIC TESTING OF HYBRID ROCKET ENGINE USING
BIOMASS WASTE

Saleh Mohammed Musaed Badi

This thesis is submitted in partial fulfilment of the requirements for the degree of
Master of Science in Mechanical Engineering

Under the Supervision of Professor Mohamed Younes El Saghir Selim

June 2022

Declaration of Original Work

I, Saleh Mohammed Musaed Badi, the undersigned, a graduate student at the United Arab Emirates University (UAEU), and the author of this thesis entitled “*Static Testing of Hybrid Rocket Engine Using Biomass Waste*”, hereby, solemnly declare that this thesis is my own original research work that has been done and prepared by me under the supervision of Professor Mohamed Younes El Saghir Selim in the College of Engineering at UAEU. This work has not previously formed the basis for the award of any academic degree, diploma or a similar title at this or any other university. Any materials borrowed from other sources (whether published or unpublished) and relied upon or included in my thesis have been properly cited and acknowledged in accordance with appropriate academic conventions. I further declare that there is no potential conflict of interest with respect to the research, data collection, authorship, presentation and/or publication of this thesis.

Student's Signature:



Date: 29.07.2022

Copyright © 2022 Saleh Mohammed Musaed Badi
All Rights Reserved

Advisory Committee

1) Advisor: Mohamed Younes El Saghir Selim

Title: Professor

Department of Mechanical and Aerospace Engineering

College of Engineering

2) Co-advisor: Jeongmoo Huh

Title: Assistant Professor and Research Fellow at the NSSTC, UAE University.

Department of Mechanical and Aerospace Engineering

College of Engineering

Approval of the Master Thesis

This Master Thesis is approved by the following Examining Committee Members:

- 1) Advisor (Committee Chair): Mohamed Younes El Saghir Selim

Title: Professor

Department of Mechanical and Nuclear Engineering

College of Engineering

Signature 


Date 14-July-2022

- 2) Member: Ki Sun Park

Title: Assistant Professor

Department of Mechanical and Nuclear Engineering

College of Engineering

Signature 


Date 19-July-2022

- 3) Member (External Examiner): Yang Zhang

Title: Professor

Department of Mechanical Engineering

Institution: University of Sheffield, United Kingdom

Signature 
Dr. E. Enajjar.

Date 22-July-2022

This Master Thesis is accepted by:

Acting Dean of the College of Engineering: Professor Mohammed Al-Marzouqi

Signature Mohamed AlMarzouqi Date August 16, 2022

Dean of the College of Graduate Studies: Professor Ali Al-Marzouqi

Signature Ali Hassan Date August 16, 2022

Abstract

This work investigates experimentally for the first time the performance of two solid biomass wastes as propellants for Hybrid Rocket Motor based on the combustion and propulsion parameters such as combustion chamber pressure, thrust force, chamber temperature, combustion characteristics, and flame length generated. The main objective of this study is to examine the performance of the proposed biomass fuels (Date stone powder and Jojoba waste powder) in comparison with typical hydrocarbon fuels. To make an accurate comparison, Paraffin Wax-based propellant was used in this study as a reference fuel to compare with biomass performance using the same testing facility and with the same operating conditions. A lab-scale Hybrid Rocket Motor with gaseous oxygen as an oxidizer operated in three ranges of volume flow rates of 80, 110, and 130 lpm. A compression device is introduced to compress the solid biomass fuel grain with a circular port along with a hot surface ignitor to ignite the system. The results suggested the expected gap in performance between biomass and hydrocarbon propellants, where a noticeable difference in performance was observed in favor of the Paraffin Wax-based propellant. However, Date Stone fuel showed slightly better propulsion and combustion characteristics compared to Jojoba. Both biomass fuels propellants have been tested in Hybrid Rocket Engine for the first time paving the way for further developments in biomass propulsion studies to be potential replacement for high pollutant and expensive hydrocarbon propellants.

Keywords: Biomass Fuel, Hybrid Rocket Motor, Paraffin Wax, Date Sone, Jojoba, Propulsion, Combustion.

Title and Abstract (in Arabic)

أختبار ثابت لمحرك صاروخي هجين باستخدام وقود عضوي

المخلص

هذا العمل يختبر عملياً للمرة الأولى أداء وقودسن حيويين في الحالة الصلبة كوقود صاروخي لمحرك صاروخي هجين بناءً على عوامل الاحتراق والدفع الصاروخي كضغط وحرارة غرفة الاحتراق وقوة الدفع الناجم الصاروخي وخصائص الإحتراق وايضا طول اللهب النجم عن الاحتراق. الهدف الرئيسي من هذه الدراسة هو اختبار أداء الوقودين المقترحين (وهما بذور التمر المطحون و الهوبهوبا) ومقارنتها مع الوقود الهيدروكربوني المتعارف عليه. من أجل الحصول على مقارنة واضحة وسليمة، تم استخدام وقود شمع البرافين في هذه الدراسة كممثل لفئة الوقود الهيدروكربوني ومرجع للمقارنة مع الوقود الجديد. تم استخدام نفس منصة التجارب ونفس الادوات ونفس ظروف التجربة في اختبار الوقود الحيوي المقترح وايضا الوقود المرجعي. تم استخدام محرك صاروخي هجين بإضافة الأوكسجين كمؤكسد غازي بثلاث معدلات تدفق حجمي مختلفة وهي 80، 110، 130 لتر/دقيقة على التوالي. تم تقديم جهاز ضغط جديد من اجل ضغط بوردرة الوقود الحيوي ليصبح متماسك عند إدخاله الى غرفة الإحتراق بحيث يكون له فجوة اسطوانية في داخله، بالاضافة لإستخدام جهاز اشعال السطح الساخن. أظهرت النتائج فجوة واضحة في الأداء بين الوقوديين الحيويين المقترحين بالمقارنة مع الوقود المرجعي وهو وقود شمع البارافين بأفضلية واضحة للوقود الأخير. إجمالاً، وقود بذور التمر أظهر أفضلية طفيفة في الدفع الصاروخي وخصائص الإحتراق بالمقارنة مع الهوبهوبا. كلا الوقودين الحيويين المقترحين تم اختبارهم كوقود صاروخي في محرك صاروخي هجين للمرة الأولى معبدة الطريق لتطورات جديدة في دراسات في الدفع الصاروخي الحيوي لتكون لبديل محتمل للوقود الهيدروكربوني الملوث للبيئة.

مفاهيم البحث الرئيسية: الإحتراق، محرك صاروخي هجين، الدفع الصاروخي، بذور التمر، الهوبهوبا.

Acknowledgements

I would like to thank my committee members and co-advisor Dr. Jeongmoo Huh for their support and guidance throughout my research work. My special thanks and gratitude to Prof. Mohamed Younes El-Saghir Seim Younia Selim who was guiding, supporting, assisting me and following up regularly in at stages of my journey at UAEU. I would like to extend my appreciation to Combustion Lab engineer who helped me during testing operations and the GP -undergraduate- students (Asma Alneyadi, Sara Alsaedi, Noura Alhemeiri and Asma AlKetbi) who designed parts of the testing facility -combustion chamber, nozzle, thrust measurement- and supervised the manufacturing process before I use it in my research.

I am especially grateful to my family parents and family who shared love and support during my studies.

Dedication

To my beloved parents and family

Table of Contents

Title	i
Declaration of Original Work	ii
Copyright	iii
Advisory Committee	iv
Approval of the Master Thesis	v
Abstract	vii
Title and Abstract (in Arabic)	viii
Acknowledgements	ix
Dedication	x
Table of Contents	xi
List of Tables.....	xiii
List of Figures	xiv
List of Abbreviations.....	xvii
Chapter 1: Introduction	1
1.1 Overview	1
1.2 Statement of The Problem.....	2
1.3 Structure of The Thesis	2
Chapter 2: Background of Literature	4
2.1 Introduction	4
2.2 Classification of Rocket Engines	7
2.3 Typical Fuels	12
2.5 Proposed Fuel Properties and Previous Use	14
2.5.1 Date Stones.....	16
2.5.2 Jojoba Solid Waste	18
2.5.3 Paraffin Wax	20
Chapter 3: Methodology	22
3.1 Rocket Geometry and Design of Components.....	22
3.2 Fuel Formulation and Preparations	27
3.3 Experimental Setup and Measurements	32
Chapter 4: Results and Discussion.....	36
4.1 Combustion Characteristics by Thermo-Gravimetric Analyzer (TGA).....	36
4.2 Propulsion Parameters.....	40
4.2.1 Chamber Pressure and Thrust Force Curve.....	40

4.2.2 Nominal Thrust, and Impulse Measurements.....	57
4.2.3 Oxidizer-Fuel Ratio.....	61
4.3 Combustion Temperature Profile for Different Fuels.....	63
4.4 Flame Visualization	65
4.5 Error Analysis	68
4.5.1 Systematic Error.....	69
4.5.2 Random Error.....	71
Chapter 5: Conclusion.....	75
5.1 Propellant Feasibility	75
5.2 Recommendations for Future Work.....	76
References	77

List of Tables

Table 1: Physical characteristics of date stone and coal	17
Table 2: Chemical Composition of Date Stones	17
Table 3: Chemical Composition of Jojoba solid waste	19
Table 4: Characteristics of propellants	20
Table 5: Paraffin Wax-based fuel composition	30
Table 6: Thermal composition for proposed fuels compared to previous studies.	39
Table 7: Reference for all results and related plots	40
Table 8: Thrust nominal, total impulse, and specific impulse for all fuels with oxidizer flow rate of 80 lpm.	59
Table 9: Nominal thrust, total impulse and specific impulse for all fuels with oxidizer flow rate of 110 lpm.	60
Table 10: Nominal thrust, total impulse, and specific impulse for all fuels with oxidizer flow rate of 130 lpm.	61
Table 11: Average, Average Deviation and Error Percentage values for all tested fuels for chamber pressure and trust force measured values.	70
Table 12: Relative error calculated for measuring devices	71
Table 13: Random error calculation	74

List of Figures

Figure 1: Representation of Solid rocket components	6
Figure 2: Nozzle profile showing throat, entrance and exit cone	7
Figure 3: Simplified diagram showing HRM components in bipropellant configuration.....	8
Figure 4: Simplified diagram showing LRM components in bipropellant configuration.....	9
Figure 5: Simplified diagram showing Hybrid Rocket Engine components	10
Figure 6: Chemical Structure of HTPB.....	13
Figure 8: Date stone solid waste sample.....	15
Figure 7: Jojoba solid waste sample.....	15
Figure 9: Schematic diagram of cross-sectional area of lab-scale.....	22
Figure 10: Closing cover showing the ignitor and the oxidizer flow line.....	23
Figure 11: Nozzle's conical shape.....	24
Figure 12: Nozzle dimensions notations.....	25
Figure 13: Rocket testing facility with cooling system.....	25
Figure 15: Compression device.....	26
Figure 16: Pressure transducer and temperature thermocouple locations.....	27
Figure 17: Propellant grains after compression process.....	28
Figure 18: Propellant grains inside the combustion chamber.....	29
Figure 19: The stand and mold for PW-based propellant.....	31
Figure 20: The propellant after being cooled and ready for the burning test.....	31
Figure 21: Schematic representing for the testing facility.....	32
Figure 22: Force Meter.....	33
Figure 23: Device used for GTA test from METTLER TOLEDO.....	35
Figure 24: Weight loss derivative for proposed biomass fuels.....	37
Figure 25: Weight loss percentage for proposed biomass fuels.....	38
Figure 26: Thrust and pressure profiles for the tested Date stone propellant with bar and Newton units respectively. The Oxidizer volume flow rate applied around 80 lpm (~ 0.96 kg/s) in 30 second burning time	41
Figure 27: Thrust and pressure profiles for the tested Date stone propellant with bar and Newton units respectively. The Oxidizer volume flow rate applied around 110 lpm (~ 1.32 kg/s) in 30 second burning time.....	42
Figure 28: Thrust and pressure profiles for the tested Date stone propellant with bar and Newton units respectively. The Oxidizer volume flow rate applied around 130 lpm (~ 1.56 kg/s) in 30 second burning time.....	43
Figure 29: Thrust and pressure profiles for the tested Jojoba solid waste propellant with bar and Newton units respectively. The Oxidizer	

volume flow rate applied around 80 lpm (~ 0.96 kg/s) in 30 second burning time. 44

Figure 30: Thrust and pressure profiles for the tested Jojoba solid waste propellant with bar and Newton units respectively. The Oxidizer volume flow rate applied around 110 lpm (~ 1.32 kg/s) in 30 second burning time. 46

Figure 31: Thrust and pressure profiles for the tested Jojoba Solid waste propellant with bar and Newton units respectively. The Oxidizer volume flow rate applied around 130 lpm (~ 1.56 kg/s) in 30 second burning time. 47

Figure 32: Thrust and pressure profiles for the tested Paraffin Wax propellant with bar and Newton units respectively. The Oxidizer volume flow rate applied around 80 lpm (~ 0.96 kg/s) in 30 second burning time. 48

Figure 33: Thrust and pressure profiles for the tested Paraffin Wax propellant with bar and Newton units respectively. The Oxidizer volume flow rate applied around 110 lpm (~ 1.32 kg/s) in 30 second burning time. 49

Figure 34: Thrust and pressure profiles for the tested Paraffin Wax propellant with bar and Newton units respectively. The Oxidizer volume flow rate applied around 130 lpm (~ 1.56 kg/s) in 30 second burning time. 50

Figure 35: Pressure profile for all tested propellants with oxidizer volume flow rate of 80 lpm (~ 0.96 kg/s). 51

Figure 36: Pressure profile for all tested propellants with oxidizer volume flow rate of 110 lpm (~ 1.32 kg/s). 52

Figure 37: Pressure profile for all tested propellants with an oxidizer volume flow rate of 130 lpm (~ 1.56 kg/s). 53

Figure 38: Thrust profile for all tested propellants with oxidizer volume flow rate of 80 lpm (~ 0.96 kg/s). 54

Figure 39: Thrust profile for all tested propellants with oxidizer volume flow rate of 110 lpm (~ 1.32 kg/s). 55

Figure 40: Pressure profile for all tested propellants with oxidizer volume flow rate of 130 lpm (~ 1.56 kg/s). 56

Figure 41: Total impulse for all fuels under GOX of 80 lpm (0.96 kg/s). 58

Figure 42: Total impulse for all fuels under GOX of 110 lpm (1.32 kg/s). 59

Figure 43: Total impulse for all fuels under GOX of 130 lpm (1.56 kg/s). 60

Figure 44: O/F ratio for all runs. 62

Figure 45: Temperature profile for tested propellants with oxidizer volume flow rate of 110 lpm (~ 1.32 kg/s). 64

Figure 46: Representation of measuring methodology for the PW flame length at an oxidizer volume flow rate of 130 lpm. Where 6.49 equals 100.4 cm. 65

Figure 47: Flame length of Date Stone propellant at 130 lpm where 2.7 equals 41.8 cm.	66
Figure 48: Flame length of Jojoba propellant at 110 lpm where 2.23 equals 34.5 cm.	66
Figure 49: Flame length representation with variant oxidizer volume flow rate for all tested propellants.	67
Figure 50: Three runs for PW-based fuel at a volume flow rate of 80 lpm (0.96 kg/s).....	72
Figure 51: Three runs for Date Stone fuel at volume flow rate of 110 lpm (1.32 kg/s).....	73

List of Abbreviations

<i>Avg</i>	Average
BD	Bulk Density (kg/m^3)
CPs	Composite Propellants
β	Nozzle Angle ($^\circ$)
DAQ	Data Acquisition
DTG	Derivative Thermogravimetric
D_c	Nozzle Entrance Diameter (mm)
D_e	Nozzle Exhaust Diameter (mm)
D_{eopt}	Nozzle Optimal Diameter (mm)
D_t	Throat Diameter (mm)
ED	Energy Density (GJ/m^3)
F_l	Flame Length (cm)
g_o	Gravity Acceleration
G_o	Propellant Mass Flow Rate (kg/s)
GOX	Oxidizer Mass Flow Rate (kg/s)
HRM	Hybrid Rocket Motor
I_s	Specific Impulse
L_c	Nozzle Converging Section Length (mm)
L_d	Nozzle Diverging Section Length (mm)

L_o	Total Nozzle Length (mm)
L_{grain}	Grain Length (mm)
\dot{m}	Mass Flow Rate
m_i	Initial Fuel Mass
m_f	Final Fuel Mass
m_{fuel}	Mass of The Fuel Consumed
m_{GOX}	Mass of The Oxidizer Consumed During Burning Time
MW	Molecular Weight (kg/mol)
NC	Nitrocellulose
NG	Nitroglycerin
O/F	Oxidizer-Fuel Ratio
PE	Polyethylene
PMMA	Poly (Methyl methacrylate)
PW	Paraffin Wax
SB	Single-Base
SRM	Solid Rocket Motor
ρ	Density (kg/m^2)
TB	Triple-Base
TGA	Thermogravimetric Analyzer
V_e	Exhaust Velocity

Chapter 1: Introduction

1.1 Overview

The story started in China thousands of years ago, as most historians suggest the black powder to be the discovery of rocket science as fireworks, where the Chinese investigated experimentally the fire-producing substances by mixing chemicals such as sulfur, charcoal, and potassium nitrate [1]. The major development took place in Europe by transferring this fireworks technology into military rockets and implementing it in two different directions: space exploration and military missiles in the mid-20th century [2]. During World War 2 in Germany, liquid propellant appeared for the first time, and a new era of research and development opened, especially for space exploration applications where most space rockets nowadays use liquid fuel.

Rocket propulsion is a wide range of systems that work on the principle of thermodynamic expansion of gas by converting the chemical to thermal energy and then into kinetic form in exhaust flow, generating a huge driving force (known as thrust) [3]. Chemical rocket propulsion, which is the concern of this study, is the application of high pressure combustion reaction of chemical types of fuel (known as propellant) associated with oxidizing chemicals (known as Oxidizers) inside the combustion chamber, resulting in expansion of the high temperature gases to produce high exhaust velocity through a converging-diverging shock area called a nozzle.

1.2 Statement of The Problem

This work proposes, for the first time, testing biomass fuels in a Hybrid Rocket Motor (HRM), following up with previous studies on burning those proposed fuels in different combustion systems and from the physical and chemical analysis of the fuels, which proved to have high heating values with attractive properties. The main goal is to make a complete comparison between the proposed fuel performance with a typical widely used one, such as paraffin wax, in a range of oxidizer flow rates. The performance parameters to be taken into consideration while comparing fuels in different oxidizer flow operations are the regression rate, thrust, chamber pressure, chamber temperature, and the size of the flame.

Based on literature studies in Paraffin Wax (PW), the mixture of PW contains stearic acid and carbon nanopowder to strengthen the mechanical properties of the mixture, while it's not the case with proposed biomass fuel. For perfect judgment of proposed fuel performance compared to typical fuels, the same facility and testing conditions were adopted for all fuels tested, including the burning time.

1.3 Structure of The Thesis

Chapter 1: The first chapter of the thesis gives an introduction to the field of the study and a general understanding of rocket science, followed by explaining the problem statement and the goal of the work, then showing what the reader should expect based on the thesis structure.

Chapter 2: The second chapter discusses the background literature of previous hybrid rocket engine experiments using various fuels as well as the classification of rocket engine systems. Furthermore, this chapter introduces common fuels and provides an

overview of related literature studies, as well as proposed new fuels and their chemical properties.

Chapter 3: The third chapter illustrates the methodology of testing by describing the testing procedure, facilities, and measurement control. Furthermore, this chapter discusses the fuel formation and preparation procedures before being installed in the testing facility to be burned.

Chapter 4: The fourth chapter focuses on results analysis and discussion by presenting the output data collected as well as describing the performance trends to draw a comparison among tested fuels.

Chapter 5: The last chapter concludes the thesis by discussing the proposed propellant feasibility and suggesting some implications, along with recommendations for future work in this field of study.

Chapter 2: Background of Literature

2.1 Introduction

Rocket propulsion systems are the leading technology that enables humans to reach space and move in space. The rocket systems were designed to produce a huge amount of power to push the payload up to pass the atmosphere cover, with small rocket engines to direct the payload to a desired position or to take place in a certain orbit. The power released at the rocket's lift-off is represented by the massive amount of gas released in a relationship between reaction force and mass ejection. The thrust equation consists of two part, the momentum thrust and pressure thrust as follow:

$$F = \dot{m} \cdot V_e + (P_e - P_o) A_e$$

Where F represents thrust, which is the reaction force, \dot{m} is the mass flow rate, V_e is the exhaust velocity, P_e is the exit pressure, A_e is the exit area and P_o is the ambient pressure. The thrust force of the rocket is a result of the thrust generated by the combustion of the propellant inside the combustion chamber before the expansion of the resulting gases through the converging-diverging nozzle. Meanwhile, the function of the nozzle is to transfer this pressure into supersonic exhaust. Along with thrust measurement, *total impulse* I_t is an important parameter for evaluation rocket engine performance where it's the thrust force integrated over the firing time:

$$I_t = \int_0^t F dt \tag{1.1}$$

With that value, it's possible to calculate the *Specific impulse* I_s where the total impulse to be divided by unit weight of propellant.

$$I_s = \frac{\int_0^t F dt}{g_o \int \dot{m} dt} \quad (1.2)$$

Where g_o is the gravity acceleration constant and \dot{m} is the mass flow rate. Since the velocity profile is difficult to measure, *effective exhaust velocity* c is assumed as uniform axial velocity of the ejected propellant and can be calculated using specific impulse as follow:

$$c = I_s g_o \quad (1.3)$$

There are many types of rocket engines depending on the fuel and oxidizer types and phase. The rocket engine's classification will be discussed in the next section. Overall, regardless of the rocket's type, there are many shared components among all shown in Figure 1.

One of the main components of the rocket engine is the propellant. The propellant could be in two different configurations, freestanding grain and case bonded grain, in addition to some central ports designed to meet the desired performance objectives. Free standing grains where the propellant grains are mounted inside a cylindrical cartridge, mostly plastic ones. In this cartridge, the grains are supported by wedges or grids to hold if fixed. However, the case-bonded grains are produced using the propellant casting method by pouring the grains directly into the mold, whose function

is to provide a strong containment for the propellant grains. Moreover, the mold could function as a thermal insulator during the combustion.

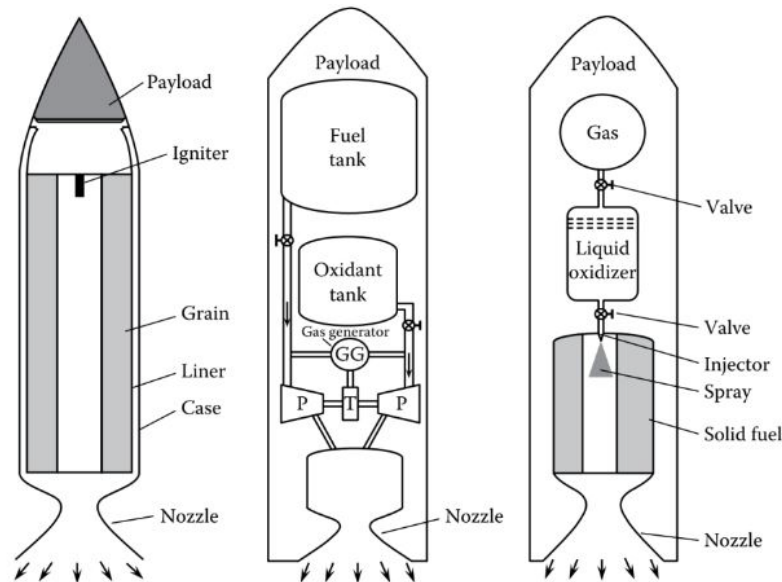


Figure 1: Representation of Solid rocket components [4]

With propellant combustion temperature ranges of approximately 1400 to 3500 K, the inner surface of the case must be provided with protection. Therefore, thermal insulation is a critical part and essential component to be installed in any rocket application to prevent any damage due to high temperatures. One of the main components that needs to be taken into consideration in a rocket's design is the diverging-converging nozzle. The nozzle shape, called the nozzle profile, consists of three major parts, as shown in Figure 2. Due to high pressure and temperature in the combustion chamber, the propeller is driven toward the nozzle, where the nozzle's entrance is the convergent zone of the nozzle. As the cross-section of the divergent zone is shrinking, it is moving to the second major zone, the throat. The throat's design specifies the operation point of the rocket engine and creates flow chock before flow expansion into the third component of the nozzle, the divergent zone. The divergent

part is responsible for increasing the exhaust gas velocity, which results in propelled improvement.

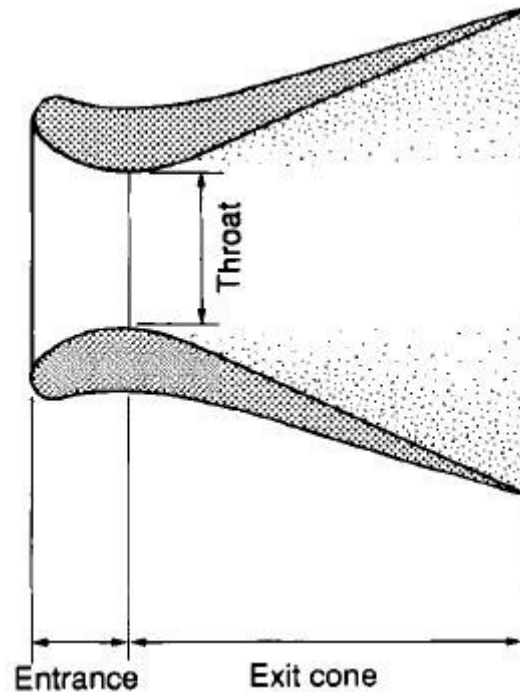


Figure 2: Nozzle profile showing throat, entrance and exit cone [5].

2.2 Classification of Rocket Engines

Based on the fuel type, rocket systems could be divided in main three paths, Liquid, Solid and Hybrid rocket propulsion. Propulsion's thermo-energy release as results of a chemical reaction between the fuel and the oxidizers [6]. Fuel and oxidizer's status of matter and arrangement are the key factor regarding classification of rockets. Based on that, fuel and oxidizers configuration inside the rocket body specifies the type of rocket system being used, Liquid, Solid, and Hybrid Rocket Engine (SRM and LRM) [5, 6]. In SRM, both fuel and oxidizers are in the solid state of matter while fuel and oxidizer are liquid in case of the LRM. Unlike typical LRM (with separate fuel and oxidizer tanks) or SRM (with solid fuel merged with its oxidizer in the same

compartment), HRMs use a solid fuel and a liquid or gaseous oxidizer separately in separate cylinders.

SRM is the first type of rocket invented and the simplest to design. By loading the mixture of solid propellant into the combustion chamber, the propellant is going to take the cylindrical shape of the chamber while waiting for the external source to ignite the substance. Although SRM is better at stability, the specific impulse of the engine is relatively lower. When the ignition takes place, the propellant starts to burn from inside and is gradually consumed till it reaches the cylinder wall to finish the propellant amount [8] as shown in Figure 3.

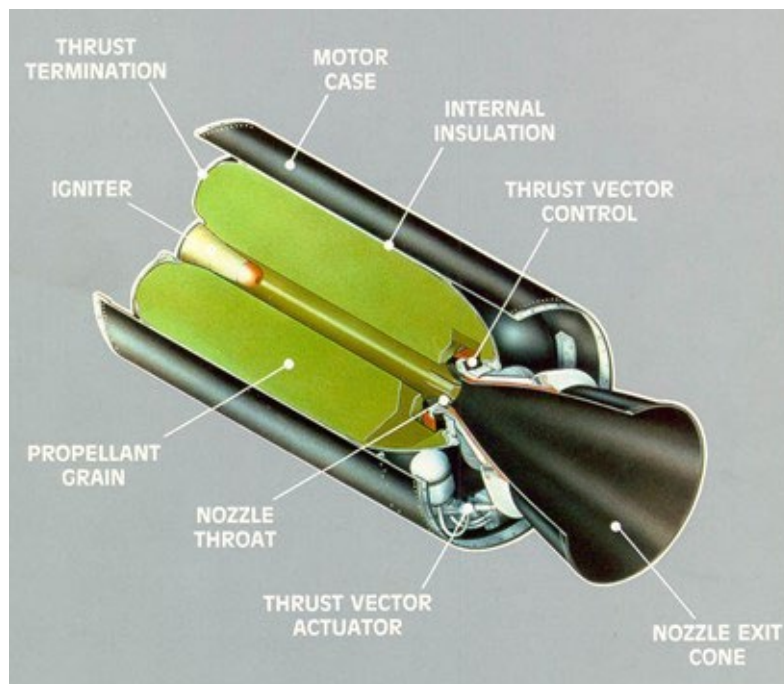


Figure 3: Simplified diagram showing HRM components in bipropellant configuration.

One of the SRM disadvantages is the lack of control over the oxidizer flow inside the combustion chamber. once the system is ignited, the combustion process can't be shut

down. As a result of that, SRM is relatively more dangerous than other types of engines if things go out of control during the operation, and most of the rocket motors are used once only. The SRM's cost is relatively lower than LRM and HRM, but the rocket components remain after fuel burning and can't be used again [6]. Unlike LRM, both fuel and oxidizer are in a liquid state where the system includes at least one tank to store propellants before injecting them through pipes into the combustion chamber using the feed mechanism.

The most common configuration of LRM is the *bipropellant* where the fuel and oxidizer are stored in separate tanks not to be mixed before entering the combustion chamber, as shown in Figure 4. Sometimes *monopropellant* is used where one tank contains the fuel and the oxidizer with one flow line toward the chamber.

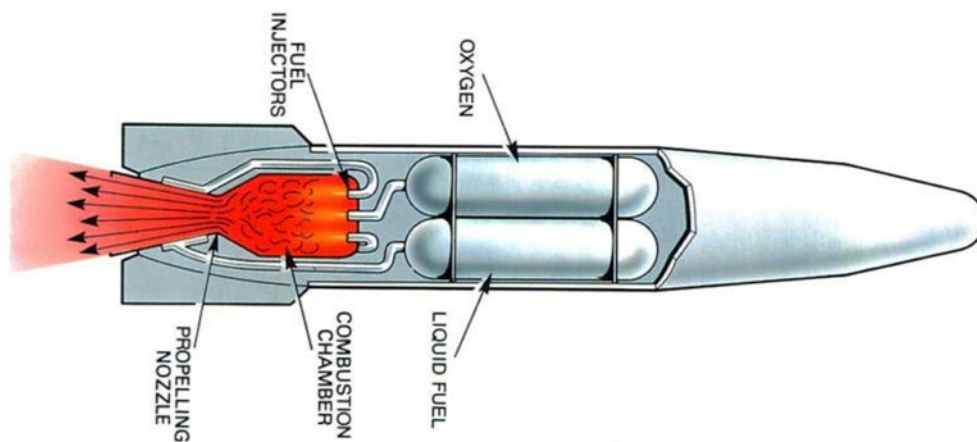


Figure 4: Simplified diagram showing LRM components in bipropellant configuration [9].

Nowadays, LRM is the most common for space rockets due to the great amount of energy produced compared to the amount of burned fuel. However, this type of rocket engine is the most complicated and most expensive. Due to the design complexity, especially for the feeding mechanism part, the system is more prone to leakage

problems, which might lead to catastrophe [8, 9]. However, when an issue takes place after ignition, it's not difficult to shut down the system by blocking the feeding line to the chamber.

The HRM system is a hybrid of SRM and LRM, with the fuel in solid form and the oxidizer in gaseous or liquid form. The oxidizer is to be stored in a tank in a certain condition depending on the oxidizer type before being injected into the chamber through a feeding line. The solid fuel grains, which take the chamber's cylindrical shape, cannot be combusted without the flow of the oxidizer as shown in Figure 5. During grain burning, a boundary layer appears as a result of reaction between the liquid oxidizer and the fuel grains, leading to fuel grain regression where it vaporizes with time. Due to the diffusion of the vaporized fuel toward the boundary layer, a flame develops in the regions of contact between the fuel and oxidizer flow, which transfers the heat into the new bottom layer of the fuel grain to burn it [12]. This cycle of regression of the solid fuel surface due to heat in a time frame is called the *regression rate*, which is one of the essential factors in judging the performance of SRMs and HRMs

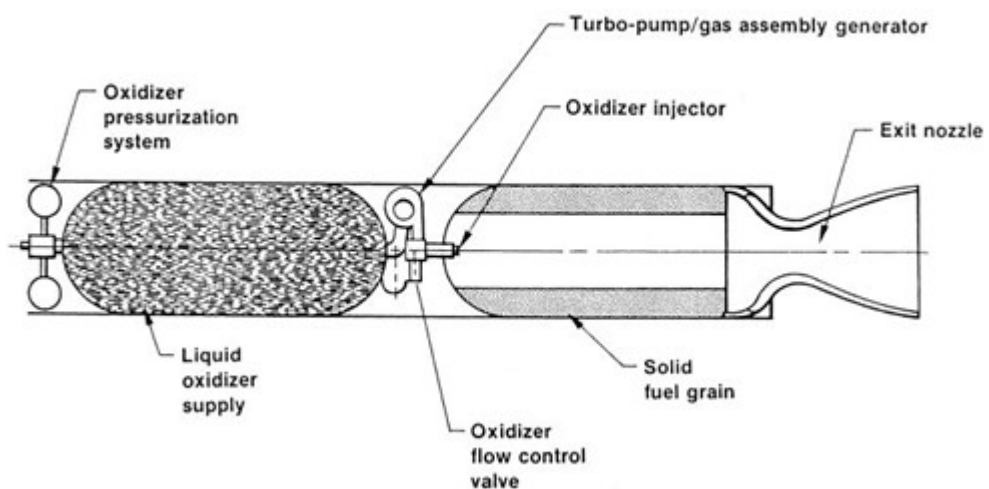


Figure 5: Simplified diagram showing Hybrid Rocket Engine components [10].

Safety is the main advantage of using HRMs compared to other systems, taking into consideration the ease of dealing with the fuel in manufacturing and transportation separately with non-explosive hazards [11-13]. Like LRMs, HRMs can be throttled by controlling the fuel feeding mechanism and shut down when needed. Moreover, throttling is easier with HRMs since only the fuel feeding line needs to be controlled compared to the complex synchronization of both fuel and oxidizer flows in LRMs [10]. The high operational cost of LRM is a real challenge due to the amount of fuel to be consumed in one mission specialty for large-scale engines such as Space Rocket Engines. In addition to fuel consumption, the HRM has only half the pipework system required for a liquid rocket motor, and therefore the cost and complexity of the system can be greatly reduced [12]. Furthermore, HRM facilities are safer in that fuel storage can be located within or near the launching site [9, 11].

Despite the many advantages of HRMs, some disadvantages are important to be studied and developed. The wide flame diffusivity in HRMs lowers the combustion efficiency by a decreasing degree of mixing [13]. Moreover, combustion efficiency can be affected by the intrinsic combustion property that combustion occurs only in the turbulent boundary layer as a diffusion flame [15]. Other factors may play a role in a performance drop, such as O/F ratio manipulation and improper ratio initiation [6]. The formation of a detached flame over the combustible surface of the grains as a result of the combustion zone's limitation to the boundary layer makes the HRMs incomplete without using a specific mechanism for mixing the fuel with oxidizer [14]. Moreover, more studies are needed to overcome combustion instability and a low regression rate for classical hybrid propellants.

2.3 Typical Fuels

Propellant choices for solid grains and fluid oxidizer are wide. A lot of varieties of gaseous and liquid oxidizers used with LRM can be adopted along with countless available solid fuels. The typical and most common types are the cross-linked rubbers such as (hydroxy-terminated polybutadiene) HTPB and plastics such as (polyethylene) PE and poly-methyl 2-methylpropenoate (PMMA). Common fuels like paraffin wax are being used recently, especially to replace low regression rate fuels, while the typical oxidizers are liquid nitrous oxide (N_2O) and pure oxygen (O_2). In terms of lab-scale testing for research, PMMA is the most used fuel, not only due to easy accessibility but also for low cost and safety reasons.

Due to wide variation, propellants are classified according to chemical composition [16]. Single-base (SB) propellant is the type of propellant that includes Nitrocellulose (NC) in its chemical structure, while Double-base (DB) propellant includes Nitroglycerin (NG) or nitric acid ester in addition to NC. However, by the addition of nitroguanidine to the DB propellant, a triple-base (TB) will be formed as the third type. Furthermore, the fourth and last types of the list are composite propellants (CPs), which contain solid oxidizer particles [17]. For the last many decades, SB propellants have been replaced by DB propellants in many applications, while CPs have become the most popular option due to rapid research development over recent years [18-20]. Apart from the chemical composition, there are many factors that need to be considered while choosing a fuel for certain applications, such as the manufacturing and mold-creating samples, regression rate, specific impulse, and mechanical properties. Among CPs, HTPB is the most common fuel because of its good mechanical properties and the amount of heat released during combustion, which

makes it resistant to senility [6]. As shown in Figure 6, the limitation of specific impulse in non-functionalized HTPB could be justified due to a lack of energetic properties in its core backbone hydrocarbon series of particles. Although using HTPB is the most common as HRM combustible, the low regression rate represents a challenge [21]. Aiming to increase the performance of HTPB in terms of the regression rate, metallic additives mixed with HTPB based blind showed promising results [17]. Moreover, HTPB faces environmental challenges due to high smoke content produced in exhaust gases. As far as fuel's regression rate is concerned, Paraffin Wax represents a better option, considering a higher regression rate compared to HTPB and 2-5 times higher than PMMA and PE.

In terms of lab-scale testing for research, PMMA is the most commonly used fuel, not only due to easy accessibility but also to low cost and safety reasons. As far as fuel's regression rate is the concern, Paraffin Wax represents a better option, taking into account a higher regression rate compared to HTPB and 2-5 times higher than PMMA and PE.

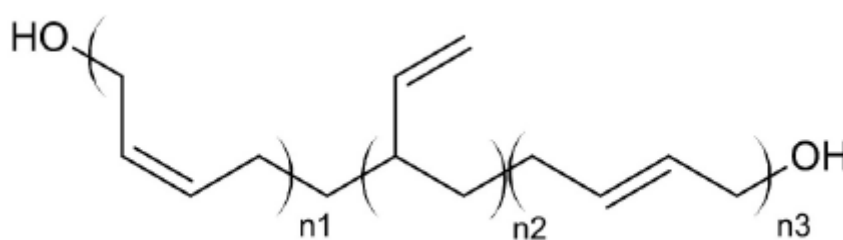


Figure 6: Chemical Structure of HTPB.

Aiming to increase the performance, a metallic particle added to the fuel grains has been tested and showed promising results in terms of increasing the combustion temperature and chamber pressure [18]. The most common particles used are Magnesium (Mg), Aluminum (Al) However, Boron (B), Ammonium nitrate (AN), and

black carbon. Furthermore, there are many additives that could be added to increase the combustion performance, such as catalysts, plasticizing agents, and curing agents [19]. However, due to the increment in fuel's molecular weight as a result of adding metal particles, a noticeable decline in specific impulse led to lower combustion efficiency.

Like fuel grains, HRM has a wide range of oxidizers to be fed into the system, such as Gaseous Oxygen (GO_2), Hydrogen Peroxide (H_2O_2), Liquid Oxygen (LO_2) and Nitrogen Tetroxide (N_2O_4). It's important to study the chemical characteristics of the fuel grains and the potential chemical compatibility with the oxidizer before choosing an oxidizer fluid to achieve the best combustion performance possible. Selection criteria of oxidizers depend on many factors such as lunch safety, availability, ease of ignition and storability [25]. LO_2 is used the most in LRM, although it one of the most active oxidizers, in some application GO_2 is being used due tower cost and safer to store and handle.

2.5 Proposed Fuel Properties and Previous Use

The world is moving forward to replace fossil fuels and hydrocarbons with green alternatives in all fields, such as power generation, transportation, and rocket propulsion. The propellants used in almost all current rocket-based applications like military or space programs have an impact on the environment at different levels. Improper handling of the fuel leads to poisoning of the ecosystem around the launch site due to chemical leakage into groundwater or blasts, in some cases due to sun heat or sudden fire. Furthermore, a considerable part of the reaction gaseous exhausts participates in the CO_2 levels to be increased in the atmosphere. Finally, gaseous

exhausts reactions with the atmosphere increase CO_2 levels [21]. Another motivation for this work is to find an easy and cheap alternative fuel for such rockets.



Figure 8: Jojoba solid waste sample.



Figure 7: Date stone solid waste sample.

Based on that, in many combustion applications, researchers have presented many alternatives, including biomass-based substances. However, no previous studies considered biomass-based fuel for rocket propulsion applications. This study provides for the first-time experimental investigation of biomass waste as a propellant in HRM application. The biomass waste propellants used are Date Stone and Jojoba solid waste. Jojoba solid waste was collected after the oil extraction process before being ground

to get a soft powder. Figure 7 and 8 show the Date Stone and jojoba propellants. More details about the proposed fuels and their properties are in the following sections.

2.5.1 Date Stones

Date Stone is one of the largest unutilized bio-resource in Middle east and North Africa, and the United Arab Emirates (UAE) for having 7% of worldwide date palm trees and being in the top list of date worldwide producers [22]. The seed represents third of the total weight of the date, with unutilized potential energy source or could be converted to valuable element in chemicals [23]. Many studies have been conducted to investigate the potential use of Date Stones in various application using different methodologies such as oil extraction, posterior of biodiesel production, thermal pyrolysis, and replacing coal in furnace combustion. Figure 8 shows the Date Stones flakes used in this experimental research work.

Many attempts to measure the heating value of Date Stone were recorded. Elnajjar et al. [24] used Bomb calorimeter to measure the heating value of Date Stone before and after the oil extraction and found it to be ranged from 28.55 MJ/kg (before liquid oil extracted) to 29.63 MJ/kg (after liquid oil extracted).

Combustion investigation of palm-date stones in a laboratory-scale furnace have been carried out by [31, 32] as an attempt to examine the physical and thermal characteristics of the date stones. While Elmay et al. [25] compared date stone finding with other palm tree residue, Al-Omari [26] tested coal within the same condition in the purpose of comparison. Many parameters were investigated such as Volatile Matter (VM), mass fraction of fixed Carbon (FC) which is the combustible content that remain

after the substance is heated and VM is scattered, Moisture (M), Ash. Table 1 represents some of the finding of both studies.

Table 1: Physical characteristics of date stone and coal.

Study (Fuel)	M (%)	VM (%)	FC (%)	Ash (%)
Elmay et al. [25] (Date stone)	6.4	74.1	17.5	1.2
Al-Omari [26] (Date stone)	7	69	23	1.0
Al-Omari [26] (Coal)	5	12	73	10

Due to higher volatile matter and lower ash content, Date Stone showed higher combustion and heat transfer rates compared to coal in the furnace application. In terms of cost and emission, Date Stones is going to save up to 40% of coal cost with little SO_x, NO_x which limited the effects on the environment and public health [27].

The chemical composition and metal concentration are essential to understand the combustion characteristic of Date Stones. Two studies investigated the chemical composition of the Date Stones were referred to and table 2 shows the comparison outcome of both ultimate analyses in terms of Carbon (C), Nitrogen (N), Oxygen (O) and Oxygen-Carbon ratio (O/C).

Table 2: Chemical Composition of Date Stones.

Attempt	C (%)	N (%)	O (%)	O/C
Sait et al. [23]	45.30	1.00	47.20	1.04
Elnajjar et al. [24]	46.26	12.45	37.91	0.82
Al-Omari [28]	48.39	0.78		

Variation in content percentages of chemical element is expected due to the variation of palm-date types and area of growth. However, the carbon and the oxygen contents are similar in all published chemical analysis of the seeds.

Many studies have been conducted investigating the feasibility of converting Date Stones to activated carbon for chemical characterization or purification needs using thermogravimetric analysis techniques [27-29, 32-33]. However, not enough detailed combustion or pyrolysis kinetics analysis studies have been performed. Experimental analysis of combustion characteristics using thermogravimetric analyzer (TGA) is performed in this work and presented in Section 4.1 with comparison with similar previous investigations from literature.

2.5.2 Jojoba Solid Waste

Jojoba (known as *Sommondisa Chinensis*) is a shrub grown in many parts of the world, especially deserts in the north Mexico and south of United States of America and some parts in Middle East and North Africa. Due to high oil content approximately 50%, it becomes widely used in the pharmaceutical industry, cosmetics, floor waxes, and many more applications [34-35]. Jojoba oil has a high energy content almost 42.4 MJ/kg which make even close to diesel fuel [33]. Furthermore, with high energy content, it released a negligible amount of SO_x and NO_x emission. In the recent years, most of the studies focused on using jojoba oil as potential biofuel either pure oil or its blends in diesel compression-ignition engines [37-43]. However, not many studies have been conducted to investigate the combustion characteristics of jojoba solid waste except for few furnaces combustion attempts. In this research work, the jojoba solid waste will be used as the solid propellant in HRM application for the first time.

Jojoba solid waste is the remaining flakes after applying the oil extraction process to jojoba fruit. Like with Date Stone propellant, knowing jojoba chemical composition will give a proper fact-based expectation of the combustion performance, taking into consideration the combustion characteristics of the propellant. Table 3 shows two

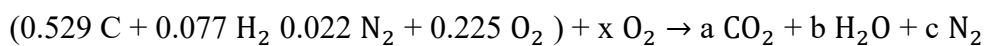
studies on the chemical components of the propellant based on examining the amount of presence of certain atoms such as Carbon (C), Nitrogen (N), Oxygen (O) and ash.

Table 3: Chemical Composition of Jojoba solid waste.

Attempt	C (%)	H (%)	N (%)	O(%)	Ash(%)
Al-Widyan et al. [31]	52.91	7.71	2.18	22.5	14.7
Selim et al. [41]	49.63	8.41	3.24	19.6	N/A

Selim et al. [41] investigated the combustion performance of jojoba solid waste in furnace application and observed that high gasification rates were observed as a result of high volatile matter of 76% and a low moisture content of 4%. Moreover, high combustion and heat transfer could be achieved with the presence of a sufficient amount of air. In this study, enough oxygen is supplied into the combustion chamber at different rates to examine the combustion performance in each condition (more details in Section 3.3).

The stoichiometric oxidizer-fuel ratio for Jojoba can be calculated starting with the chemical equation as follows:



By solving the equation, $x = 0.381$

Thus, O/F stoichiometric:

$$\frac{0.381 * 32}{0.529 * 12 + 0.077 * 2 + 0.022 * 28 + 0.225 * 32} = 5.459$$

O/F stoichiometric = 5.459

2.5.3 Paraffin Wax

The experimental investigation of paraffin wax as a potential propellant dates back to the 1950s in the United States of America [42]. During the past years, the focus on testing the propellant was focused on the reinforcement of the fuel formulation, implementing a variation of additives to improve combustion performance, and studying the ballistic effects of the fuel's entrainment [12, 46]. Unlike most typical hydrocarbon fuels, Paraffin Wax propellant behaves as a brittle material. However, because of its poor mechanical strength, it made it harder to prevent structural damage during grain fabrication, handling, casting, and transformation [44]. In practical applications, the mechanical properties of Paraffin-based propellant are usually modified by adding additive components to avoid internal and surface rips and micro-cracks that may affect the combustion performance of the fuel [45] or by blending it with thermoplastic polymers [49, 50]. Moreover, Table 4 below indicates average PW thermal properties compared to PE such as Melting point, Density (ρ), and Molecular Weight (MW).

Table 4: Characteristics of propellants [48].

Propellant	Melting Point $^{\circ}\text{C}$	Density Kg/m^3	Molecular Weight Kg/mol
Paraffin Wax	59-66	920	394
Polyethylene	104	918	96000

The high regression rate of paraffin wax is due to entrainment of the paraffin droplets with portions of vaporized paraffin into the flame, which results in an increase in the amount of fuel in the combustion zone [49]. However, Kim et al. [50] observed that some vaporized droplets leave the combustion zone unburned. To solve this problem,

it was suggested to use a small amount of polymeric binder to slow the paraffin droplet release [51]. PW-based propellant is the reference fuel in this study to examine the performance of the proposed biomass propellant in terms of thrust generated, regression rate, pressure and temperature profiles, and flame length measurement.

Chapter 3: Methodology

This chapter covers the testing and measurement methods adopted in this experimental investigation to study the problem statement mentioned earlier. The first section of this chapter will discuss the testing facility, including the lab-scale HRM, the cooling system, and the design and manufacturing process for some parts. The second section covers the most important part, which is the grain preparation for the firing test. Furthermore, the section will introduce a new compression system used for compressing the grain before installing it inside the combustion chamber for firing. Finally, the third section concerns the procedure of carrying out the testing, starting by describing the oxidizer feeding, monitoring, and measurement systems and ignition system. This section will present the methodology of combustion characteristic investigation using the TGA test and will present the results analysis method to be implemented to analyze the data collected.

3.1 Rocket Geometry and Design of Components

For this project, the focus is on fuel testing. Therefore, the testing facility manufactured by undergraduate students is to be used with some modifications. The design of the rocket engine might not meet the rocket design standards, but the same setup will be

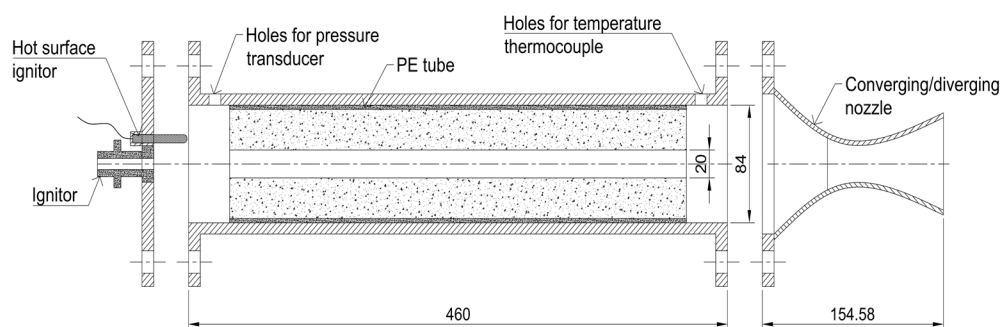


Figure 9: Schematic diagram of cross-sectional area of lab-scale.

used for all fuels, which applies the same conditions and limitations, resulting in a fair comparison under the same circumstances.

Figure 9 shows a schematic diagram for the cross-section of rocket motor components. The cylinder where the combustion is taking place was made of stainless steel to withstand the high pressure and temperature conditions, preventing failure and meeting safety needs. The cylinder length is 460 mm with an inner diameter of 84 mm and a 5 mm thickness. Two holes were made for the oxidizer feeding system and the ignitor through the closing cover, which was made from stainless steel as shown in Figure 10. To connect the cylinder with the nozzle and the closing cover, two flanges were used with a rubber ring to prevent pressure leakage to atmosphere.



Figure 10: Closing cover showing the ignitor and the oxidizer flow line.

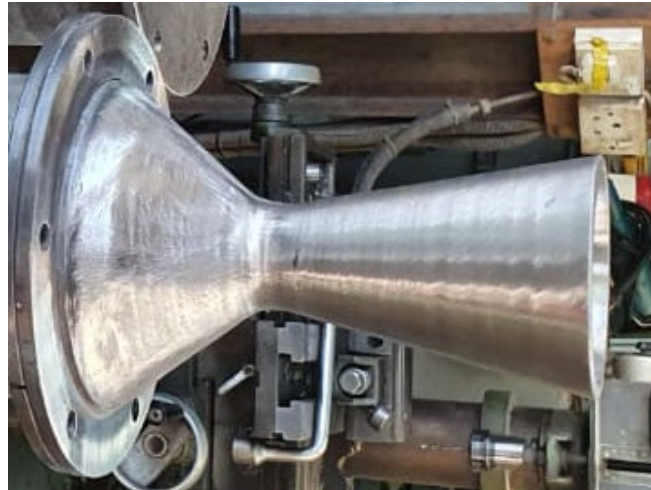


Figure 11: Nozzle's conical shape.

Like the combustion cylinder and closing cover, the converging-diverging nozzle was made of stainless steel, which makes it easy to handle during manufacturing. The nozzle shape is conical, as shown in Figure 11, with a total length (L_o) of 154.58. The nozzle consists of converging and diverging zones separated by a throat. The length of the converging part of the nozzle (L_c) is 54.84 mm, where the length of the diverging part (L_d) is almost 99.74 mm. The throat is the narrowest part where the flow changes from subsonic to supersonic and is a converging-diverging nozzle. In this application, the throat diameter (D_t) is 19.49 mm. One of the most critical parts in nozzle design is choosing the angles of convergence and divergence. The converging angle (β) in this case is 35° while the diverging angle (α) is 12. On the basis of converging-diverging angles, the entrance diameter (D_c), exist diameter (D_e) and optimum exit diameter (D_{eopt}), are 84, 55.10 and 60.48 mm, respectively. Notations are illustrated in Figure 13.

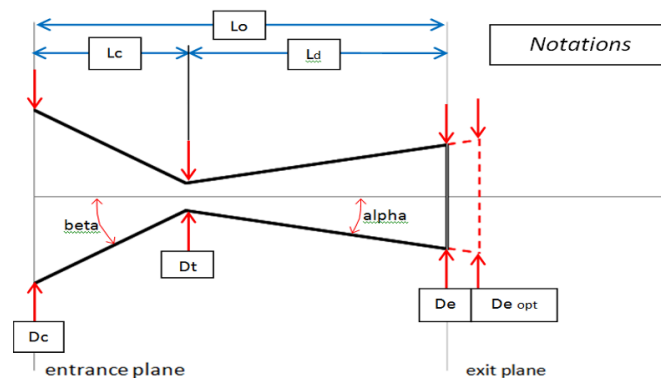


Figure 12: Nozzle dimensions notations.



Figure 13: Rocket testing facility with cooling system.

Due to high oxidizer flow, a high temperature was expected inside the combustion chamber. To prevent damage from heat, an air-cooling system was needed. By using an air blower, a forced convection was applied to cool the outer surface of the chamber. The air flow is to be directed to move towards the nozzle covering the cylinder at 360 degrees as shown in Figure 14. To keep the air constrained around the cylinder moving in hollow space, a cylindrical-shape thin aluminum shell is placed around the combustion cylinder with 5 mm of space in between. The blower was placed below the rocket testing stand where the air flow entering the cooling space through a small

hole made at the bottom of the aluminum shell and leaving it through many holes near the nozzle, as seen in Figure 15.

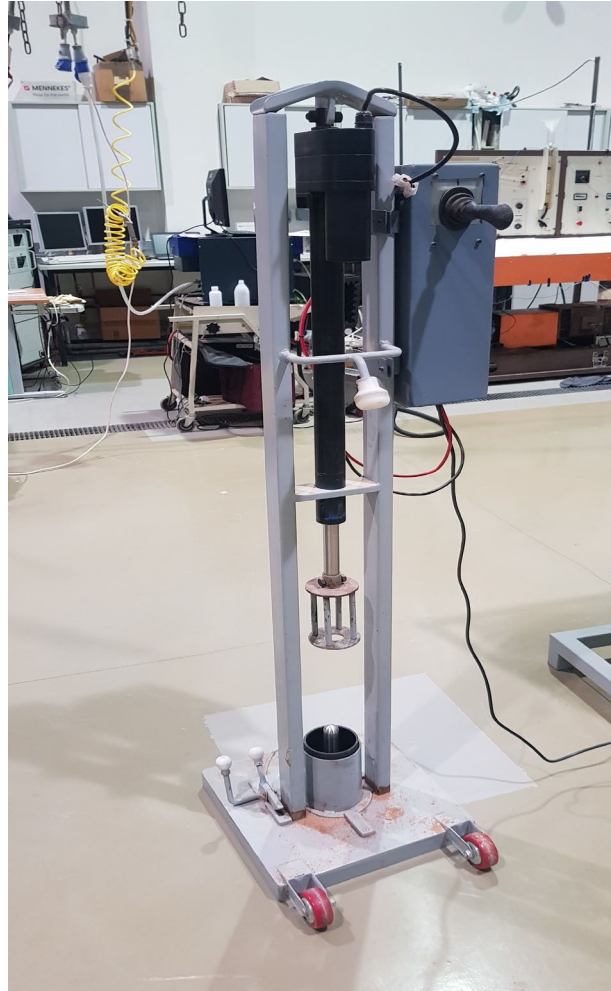


Figure 14: Compression device.

The biomass grains proposed in this research cannot be inserted directly into the combustion chamber due to their weak mechanical structure. Therefore, a compression device has been designed and manufactured to be used for strengthening the substance structure to avoid any collapse that could lead to losing the standard shape of the grains with circular port needed to perform the test. The compression device consists of a base for the grain's mold to be placed on and a strong automated arm to compress the substance using an electric actuator, as shown in Figure 16.

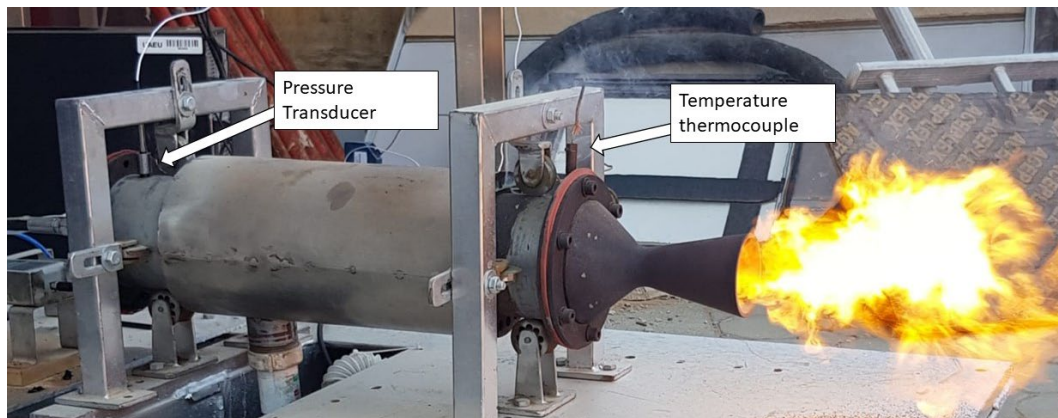


Figure 15: Pressure transducer and temperature thermocouple locations.

The compression device's work is explained in detail in Section 3.2. Having coherent grains with proper ports for the oxidizer flow helps to have a better understanding of the regression rate of the grains and the thrust generated. Thrust measurement is one of the key factors in judging the performance of the propellant. For the thrust measurement, a force meter was used to measure the rocket thrust by transferring the data to a PC through a USB cable. K-type thermocouple was used to measure the temperature inside the combustion chamber and was placed 1.5 cm away from the nozzle. Meanwhile, a piezoelectric pressure transducer was placed 3 cm away from the closing cover at the ignition side, sensing the pressure inside the combustion chamber as shown in Figure 17.

Hot surface ignition has been used to ignite the grains. Before igniting, a small piece of ethanol-enriched tissue was inserted close to the fuel, making sure the tissue is in contact with the hot surface ignitor to ensure enough heating energy is released for proper ignition condition.

3.2 Fuel Formulation and Preparations

Different manufacturing processes have been adopted for each biomass and PW-based fuel for the purpose of making proper and high-quality test fuel grain samples. Before

starting biomass fuel preparations, the moisture content was decreased by spreading the grain under the moon sun for 3 hours. The procedure of molding Date Stone and Jojoba grains requires manufacturing a strong compressing machine to make sure coherent grains are produced and a polyethylene mold to contain the grains during the compression process and inside the combustion chamber. Figure 18 shows the grains after being compressed. Then Figure 18 shows the grains after removing the metal rod and inserting them into the combustion chamber. The compression force used was designed to compress the fuel strongly until it's solid enough to allow smooth cylindrical rod removal.



Figure 16: Propellant grains after compression process.



Figure 17: Propellant grains inside the combustion chamber.

To fill most of the combustion chamber, 3 pieces of 12 cm long polyethylene molds were used to hold the compressed grains and were filled fully before ensuring all molds were inside the combustion chamber. Each mold was filled with fuel grains before placing it into a mold holder with a circular metal rod in the middle, shaping the circular slot in the fuel grains. Then compression took place, pushing the grains down by automated arm force using an electric actuator. Once the mold is full and well-compressed, the smooth metal rod is removed gently (a sample is shown in Figure 18). By repeating the same steps three times for three molds, the fuel grains are ready to be loaded into the chamber.

Because paraffin wax has poor mechanical properties, an PW-based propellant was created by combining PW with stearic acid (Octadecanoic acid) and carbon nanopowder in the percentages shown in Table 5. The Stearic acid used with PW-based propellant is weak carboxylic acid mixed with Paraffin Wax for the purpose of enhancing PW mechanical properties by decreasing its fragility [52]. Moreover, the

carbon nanopowder used in the mixture improves the radiative heat transfer taking place between the grain surface and the flame zone [14, 57-58].

Table 5: Paraffin Wax-based fuel composition.

Ingredient	Mass fraction %	Density
Paraffin Wax	87	893
Satiric Acid	10	850
Carbon Nanopowder	3	2130
PW Binder	100	≈ 920

Unlike biomass grains' manufacturing procedure, no compression device took place while producing PW-based fuel. The adopted manufacturing procedure could be summarized as follows:

1. Following the specific composition ratio stated in Table 5, a total of 2.5 kg of fuel mixture was placed in the Pyrex breaker.
2. Heating the mixture using a hot plate heater with a magnetic stirrer at a temperature of 80°C till the mixture is melted completely.
3. Keeping the magnetic stirrer spinning to mix it for 20 minutes.
4. Pouring the mixture gently into the mold and waiting for 2 hours for the fuel to be cooled. Figure 19 shows the mold with its stand.
5. Removing the metal rod and inserting the fuel into the combustion chamber.



Figure 18: The stand and mold for PW-based propellant.



Figure 19: The propellant after being cooled and ready for the burning test.

3.3 Experimental Setup and Measurements

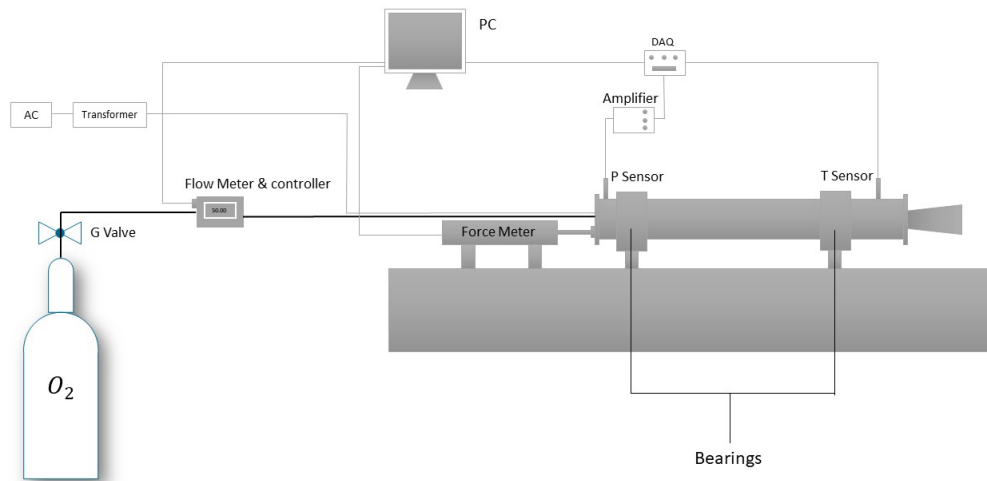


Figure 20: Schematic representing for the testing facility.

The static tests were conducted using Lab-scale HRM facility as shown in the schematic representation in Figure 21. The system mainly consist of Lab-scale HRM, gaseous oxygen feeding system, hot surface ignitor, K-type thermocouple and pressure transducer, amplifier, and data acquisition (DAQ) system, force measuring device, gas flow meter and controller. The ignition system needed 120 V power supply; therefore, a transformer has been used to reduce voltage from 240 V to 120 V. The combustion pressure was continuously measured by AVL piezoelectric pressure transducer coupled with Kistler charge amplifier and DAQ linked with a LabVIEW software that could collect the data at the rate of 10 kHz and store it in the computer for offline analyses. Kistler charge amplifier function is to convert electric charges into voltage output and calibration of pressure transducer was used to convert to pressure unit. The delay time of ignition was around 3 second were the oxidizer flow operated accordingly. The

digital force meter used was attached to the rocket and set to zero before starting the test.



Figure 21: Force Meter.

Aiming to have precise thrust measurement, a smooth wheel bearing was placed around the cylindrical combustion chamber in two parts as shown in the schematic diagram Figure 21. In addition, temperature measuring thermocouple was placed inside the combustion chamber close to the nozzle where the maximum temperature is expected to locate. High compressed oxygen cylinder was used to feed the system with the needed oxygen flux. The volume flow rate of the oxidizer was measured and controlled by Sierra smartTrak50 flow meter and controller with digital screen to show the flow reading and linked with software to control the flow rate from PC. At the

beginning of each run the oxygen gate was opened for the oxidizer to enter the combustion chamber with very low flow rate of 10 lpm for 3 seconds initially to make sure there is enough oxidizer before igniting the system. After 3 seconds ignition takes place, and the oxygen valve was for the amount desired of oxidizer to enter the combustion chamber. The rocket firing was selected to shut down after 30 seconds from ignition by closing the oxygen valve by switching flow rate to 0 lpm through the controlling software. To measure the Oxidizer/Fuel (O/F) ratio, the grain mass for each fuel was measured at the beginning and the end of each run. The first round of runs consisted of nine runs (three runs for each propellant) with a run duration of 30 seconds, measuring thrust force and combustion chamber pressure profiles, while the second round consists of three runs with durations of five, seven, and eight for PW, Date Stone, and Jojoba, respectively. The parameters and conditions were kept constant to achieve a precise and clear comparison between the three fuel types tested. For each fuel, three runs have been performed based on the oxidizer volume flow rate, starting with 80 lpm, then 110 lpm, and 130 lpm. By repeating the runs for each fuel, a total of 9 runs with measurements to be analyzed and discussed in Chapter 4.

The PW-based propellant is the reference fuel used in this study to examine the performance of the proposed biomass propellant in terms of thrust generated, pressure and temperature profiles, and flame length measurement.



Figure 22: Device used for GTA test from METTLER TOLEDO.

Similar testing conditions (i.e. burning duration, grain size, and oxidizer mass flow rates... etc) were applied for all propellant testing. Before testing, the thermal characteristics of biomass propellants were investigated using a Thermogravimetric Analyzer (TGA), as shown in Figure 23. Flame length was measured using a photo reference-scaling technique and was plotted for all proposed propellants with different oxidizer mass flow rates.

Chapter 4: Results and Discussion

In this chapter, the combustion characteristics, chamber pressure, and thrust profile of the proposed propellants are reported and discussed. The first section will compare the TGA tests and combustion properties of biomass grains to previous studies reported in Chapter 2. The second section will discuss the combustion chamber pressure and thrust force profiles for all proposed fuels. Each fuel will be tested under three conditions of oxidizer volume flow rates of 80, 110, and 130 lpm. The profiles will be presented in line graphs showing the profile trend and discussing the value and stability under each condition. Moreover, the oxygen/fuel ratio will be discussed and presented in one plot comparing all propellants under different oxygen volume flow rates. The third section will report the results for the temperature profile inside the combustion chamber for the second round of testing for a longer burning period. Finally, the last section will present a visualization of flame and report flame length for all fuels. A simple and creative methodology of scaling tool to be presented for measuring the flame length before plotting all the data in one graph for comparison purposes. A proper explanation will be provided to illustrate the finding and link the combustion performance for each fuel with the relative combustion characteristics discussed in Section 4.1.

4.1 Combustion Characteristics by Thermo-Gravimetric Analyzer (TGA)

Taking into consideration that this is the first time for the proposed biomass fuels to be burned in a rocket engine application, it was important to carry out preliminary Thermo-Gravimetric Analysis by TGA. Several previous studies were conducted to examine the combustion and pyrolysis properties of Date Stone as a propellant and

have been discussed in Chapter 2. No previous studies have been found for TGA analysis of the Jojoba solid substance.

Prior to propulsion testing, TGA tests for proposed propellants were carried out to investigate the combustion and pyrolysis characteristics of the proposed propellant samples. The device used for the experiment was the METTLER TOLEDO TGA2, with a fixed heating rate of 10 °C/min. The temperature range was from 25°C to 900°C under a Nitrogen (N₂) environment. The initial mass of the samples placed in the furnace chamber was 10.5 mg. The sample is to be heated and lose mass during the process to reach 900°C, as a result, a plot for the weight loss derivative as a derivative thermogravimetric (DTG) curve is presented in Figure 24, while the weight loss percentage with respect to temperature for both substances is presented in Figure 25.

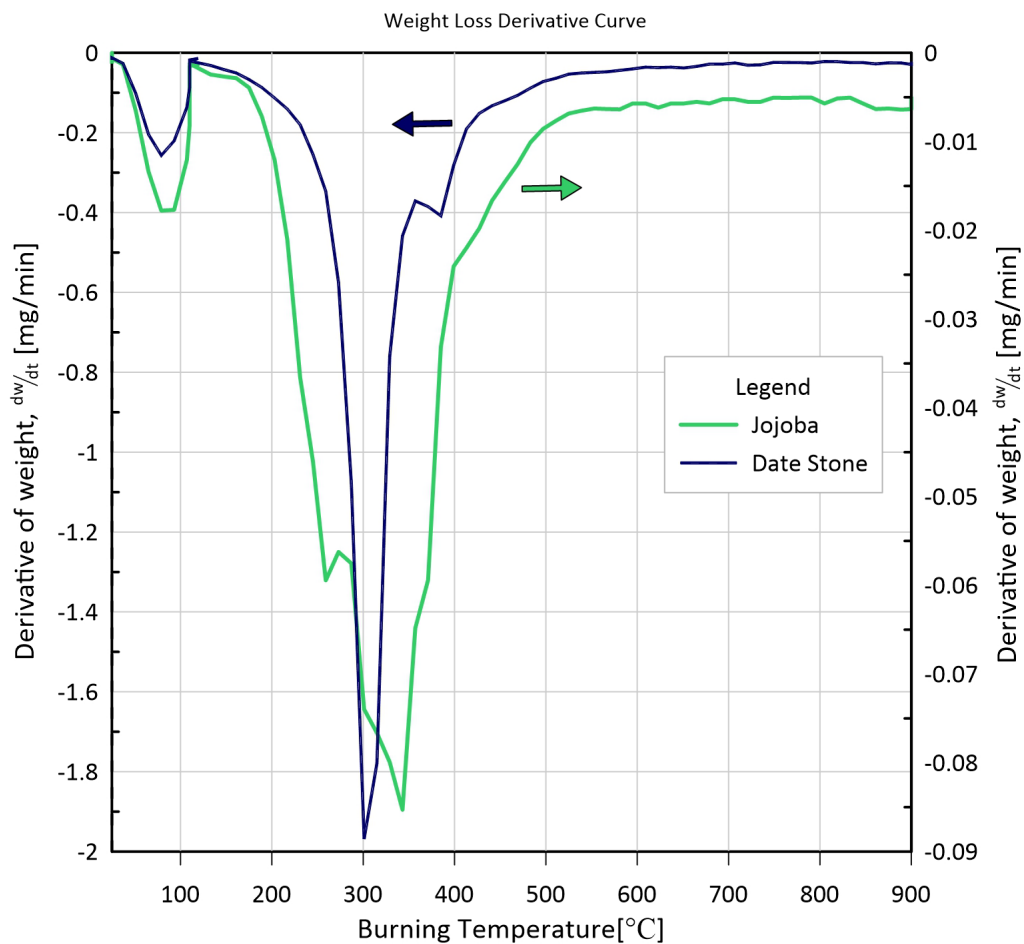


Figure 23: Weight loss derivative for proposed biomass fuels.

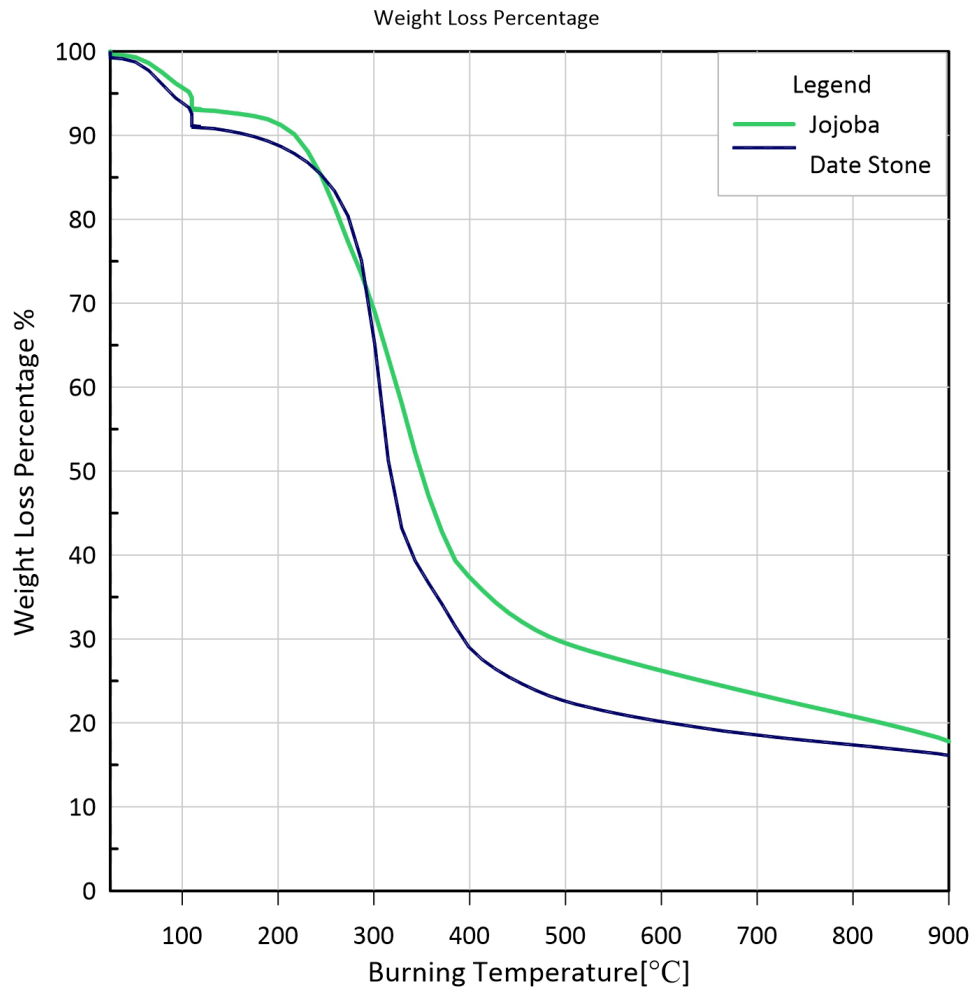


Figure 24: Weight loss percentage for proposed biomass fuels.

For both Date Stone and Jojoba, the results showed a major weight drop after 200°C, similar to previous studies [23, 27-28, 52]. However, the greatest weight loss for the Date Stone substance was at 302°C, while jojoba lost most of the weight at 344°C. In general, the range of the highest conversion and reaction was from 150°C to 500°C for both Date Stone and Jojoba. This shows that Date Stone will convert to a volatile substance faster than Jojoba solid biomass, which gives an indication of the difference in combustion nature of both fuels. From the beginning till reaching 900°C, similar trends appeared for both substances. However, a greater amount of date stone (89%) was consumed at the point of reaching 900°C while only 79% of jojoba was consumed

at that same temperature. Furthermore, till the end of the test, the ash remained for Date Stone was almost 6.44 mg compared to 20.7 mg in the jojoba case, which shows the completeness of combustion of Date Stone compared to Jojoba. Based on the weight percentage plot in Figure 25, a proximity analysis was performed to determine Moisture (M), Volatile Matter (VM), Fixed Carbon (FC), and Ash. These results were compared to results from literature discussed in Section 2.5, as may be seen in Table 6.

Table 6: Thermal composition for proposed fuels compared to previous studies.

Study (Fuel)	M (%)	VM (%)	FC (%)	Ash (%)
Elmay et al. [25] (Date stone)	6.4	74.1	17.5	1.2
Al-Omari [26] (Date stone)	7	69	23	1.0
Current study (Date Stone)	8.5	52.6	32.5	6.4
Current study (Jojoba)	6.8	45.8	26.7	20.7

Data in Table 6 reveals that Jojoba contains less moisture, volatile matter, and fixed carbon compared to Date Stone. However, Jojoba contained significant amounts of ash exceeding 20%, while Date Stone recorded only 6.4%. This test showed that the Date Stone biomass has higher moisture, fixed carbon, and ash while a lower volatile matter was recorded compared to previous studies listed in the above table.

The next section will discuss the combustion chamber pressure and thrust profiles for round 1 of testing where the tests were operated within 30 seconds of burning before shutting down by decreasing the oxidizer volume flow rate to 0 lpm via controlling software. The combustion chamber profiles for round 2 testing will be discussed in Section 4.3. Table 7 summarizes the details of tests conducted and shows the corresponding figure numbers.

Table 7: Reference for all results and related plots.

	Fuel (GOX), lpm	Period	Thrust	Pressure	Temp
Round 1	Date Sone (80)	30 s	Fig (26)	Figure (26)	
	Date Sone (110)	30 s	Fig (27)	Figure (27)	
	Date Sone (130)	30 s	Fig (28)	Figure (28)	
	Jojoba (80)	30 s	Fig (29)	Figure (29)	
	Jojoba (110)	30 s	Fig (30)	Figure (30)	
	Jojoba (130)	30 s	Fig (31)	Figure (31)	
	Paraffin Wax (80)	30 s	Fig (32)	Figure (32)	
	Paraffin Wax (110)	30 s	Fig (33)	Figure (33)	
	Paraffin Wax (130)	30 s	Fig (34)	Figure (34)	
	All Fuels (80)	30 s	Fig (38)	Figure (35)	
	All Fuels (110)	30 s	Fig (39)	Figure (36)	
	All Fuels (130)	30 s	Fig (40)	Figure (37)	
Round 2	Date Stone (110)	7 mins			Figure (47)
	Jojoba (110)	8 mins			Figure (47)
	Paraffin Wax (110)	5 mins			Figure (47)

4.2 Propulsion Parameters

The propulsion parameters which determine the performance of the fuel tested in this rocket engine application are chamber pressure, nominal thrust, total impulse, specific impulse, and O/F ratio.

4.2.1 Chamber Pressure and Thrust Force Curve

Thrust-time profile is one of the most important parameters for evaluating the rocket engine's performance. The thrust was measured for each run for three different flow rates as mentioned earlier.

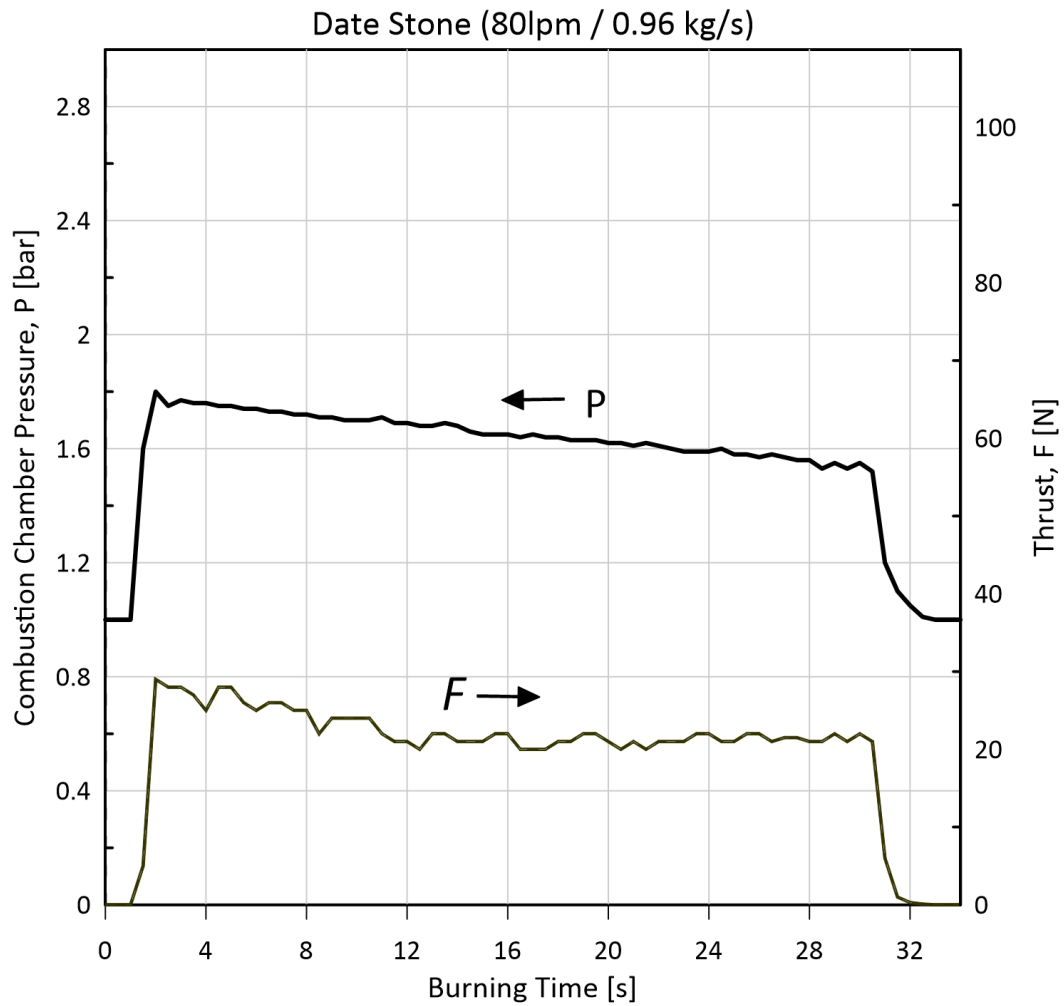


Figure 25: Thrust and pressure profiles for the tested Date stone propellant with bar and Newton units respectively. The Oxidizer volume flow rate applied around 80 lpm (~ 0.96 kg/s) in 30 second burning time.

Figures 26, 27, and 28 show pressure and thrust profiles for Date Stone propellant combustion at three oxygen volume flow rates of 80, 110, and 130 lpm, respectively.

Figure 26 shows the performance of the combustion chamber pressure and thrust force under an 80 lpm oxidizer volume flow rate (0.96 kg/s mass flow rate). While thrust force increased to 28 N then fluctuated around 25 N throughout the testing time before it dropped to 0 N, the pressure first increased to 1.8 bar then decreased steadily till the end of the experiment before it reached atmospheric pressure. By increasing the

oxidizer volume flow rate to 110 lpm in the second experiment, Figure 27 clearly shows an increment in the pressure and thrust values. The thrust increased to 27 N while the pressure reached 1.85 bar and then reduced at a slower rate. Also, the thrust did not exhibit fluctuations similar to the case of 80 lpm.

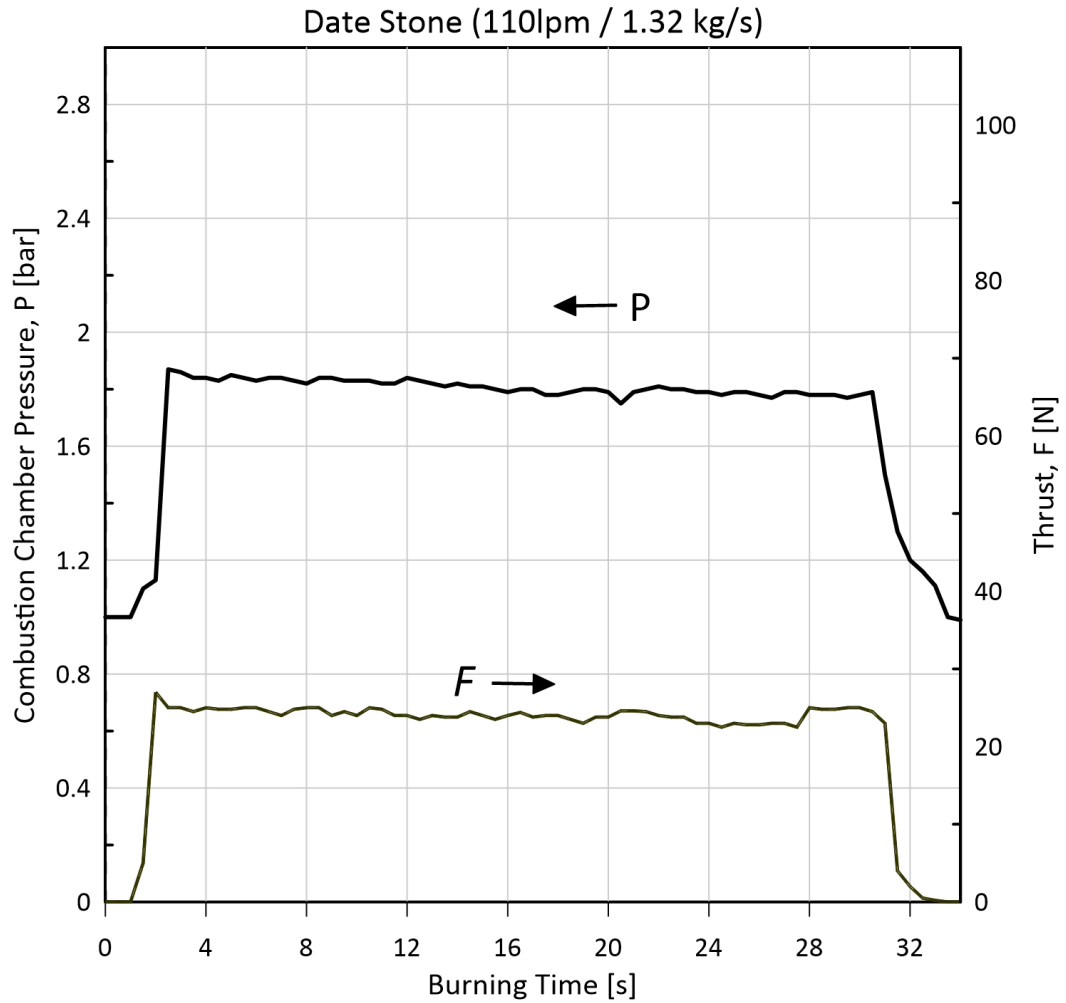


Figure 26: Thrust and pressure profiles for the tested Date stone propellant with bar and Newton units respectively. The Oxidizer volume flow rate applied around 110 lpm (~ 1.32 kg/s) in 30 second burning time.

Similarly, the improvement in pressure and thrust trend continues at a higher oxidizer volume flow rate of 130 lpm as shown in Figure 28. The thrust has increased to reach almost 40 N and the pressure has increased to 2.29 bar. Both the pressure and the thrust profiles are more stabilized.

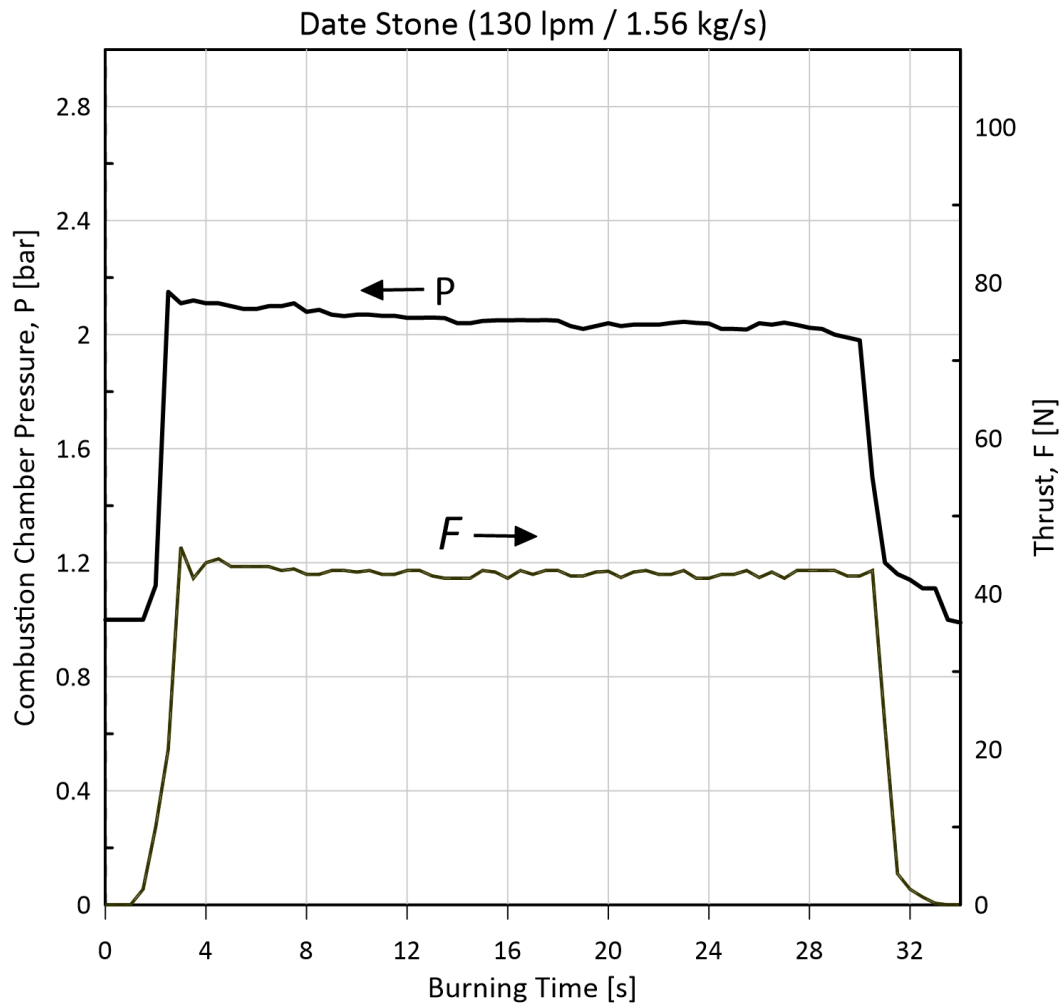


Figure 27: Thrust and pressure profiles for the tested Date stone propellant with bar and Newton units respectively. The Oxidizer volume flow rate applied around 130 lpm (~ 1.56 kg/s) in 30 second burning time.

In general, the tests of Date Stone propellant shown in Figures 26, 27, and 28 illustrate a coherent increment increase in the combustion pressure and thrust force as the oxidizer volume flow rate was increased. In addition, it's worth pointing out the

improved stability of the performance with the increase in the oxidizer volume flow rate from 80 to 130 lpm.

Figures 29, 30, and 31 show pressure and thrust profiles for Jojoba solid waste propellant combustion at three oxygen volume flow rates of 80, 110, and 130 lpm, respectively.

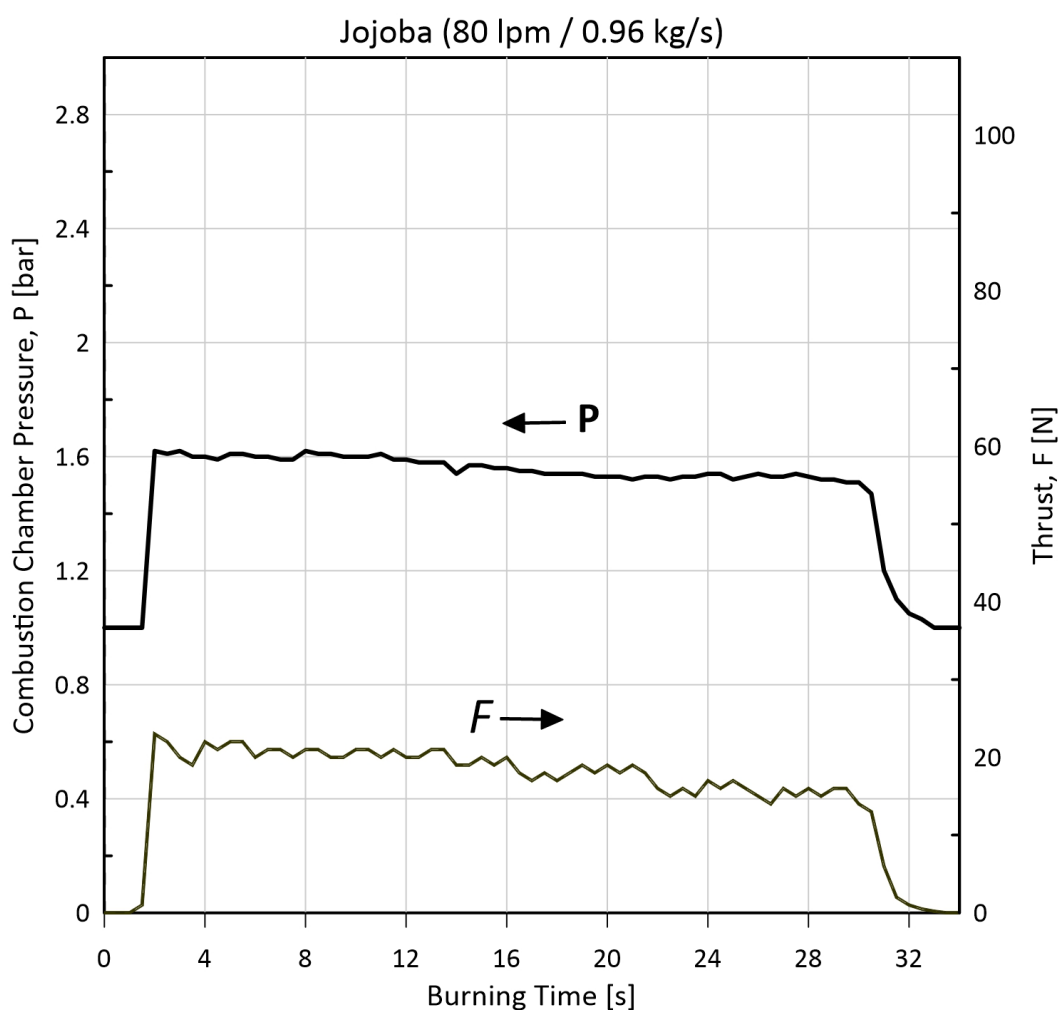


Figure 28: Thrust and pressure profiles for the tested Jojoba solid waste propellant with bar and Newton units respectively. The Oxidizer volume flow rate applied around 80 lpm (~ 0.96 kg/s) in 30 second burning time.

Figure 29 shows the performance of combustion chamber pressure and thrust force under an 80 lpm oxidizer volume flow rate (0.96 kg/s mass flow rate). While the thrust force increased to 23 N and then fluctuated around 22 N for 15 seconds. A notable fluctuation took place till the end of the run. Meanwhile, the pressure first increased to 1.65 bar then decreased steadily till the end of the experiment before it reached atmospheric pressure. Similar to the Date stone propellant case, by increasing the oxidizer volume flow rate to 110 lpm at the second experiment, Figure 30 shows an increase in pressure and thrust values. The thrust increased to 33 N while the pressure reached 1.75 bar. Also, the thrust exhibits less fluctuation like the low flow rate of 80 lpm as shown in Figure 29. Moreover, it is notable that the combustion pressure and thrust performance of jojoba in this test showed slightly lower values compared to date stone propellant under the same oxidizer flow rate condition. Jojoba showed a similar fluctuation in thrust profile to Date Stone. However, the Date Stone thrust profile maintained the same average value till the end of the experiment, while the Jojoba thrust had a considerable drop after 20 s of burning. The fifth test was the jojoba propellant at 110 lpm, as shown in Figure 30. As expected, there is an obvious and consistent increment in pressure and thrust profiles with higher oxidizer volume flow rate.

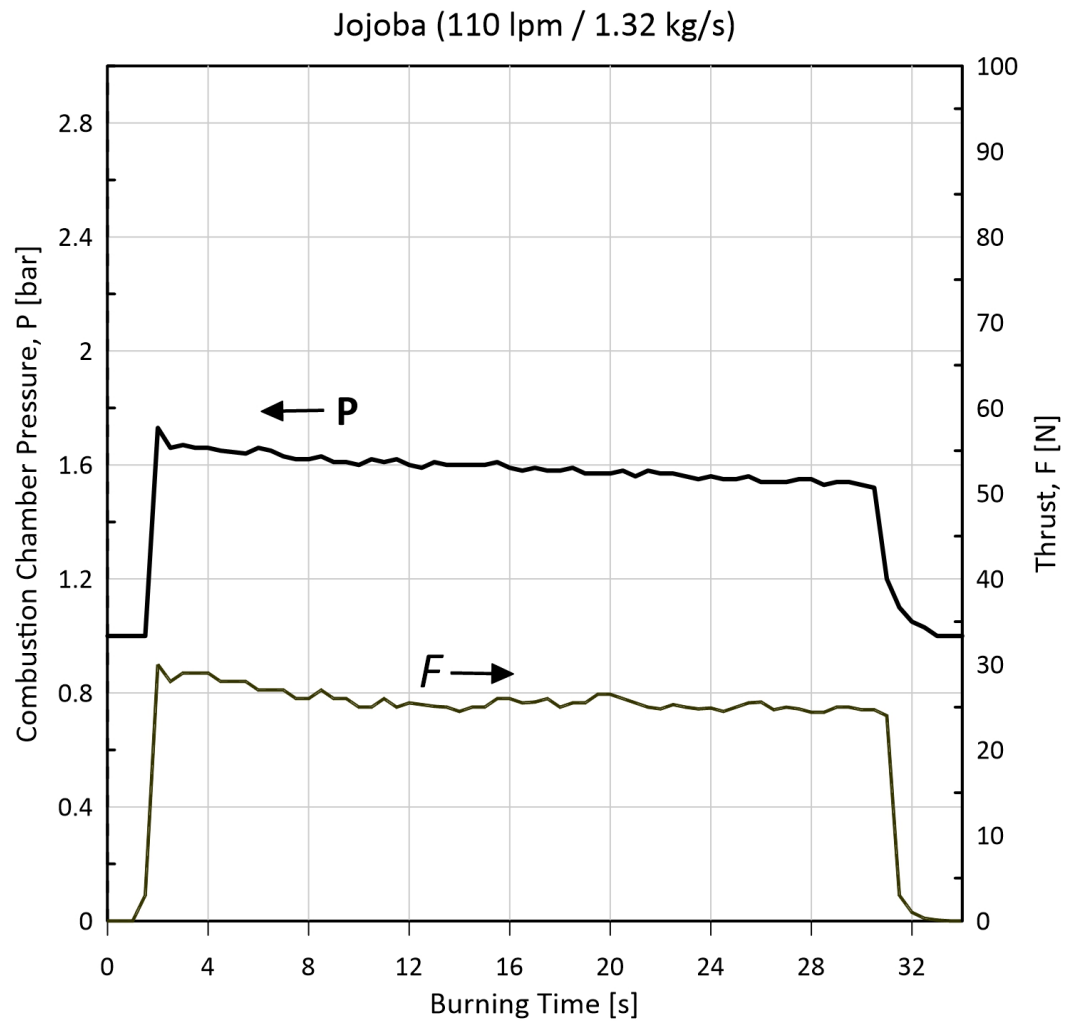


Figure 29: Thrust and pressure profiles for the tested Jojoba solid waste propellant with bar and Newton units respectively. The Oxidizer volume flow rate applied around 110 lpm (~ 1.32 kg/s) in 30 second burning time.

Jojoba at 110 lpm showed more stability in the thrust profile, while a similar trend showed a higher value for the combustion pressure profile. By increasing the oxygen volume flow rate to 130 lpm in the jojoba's third experiment, the performance showed interesting results as presented in Figure 31.

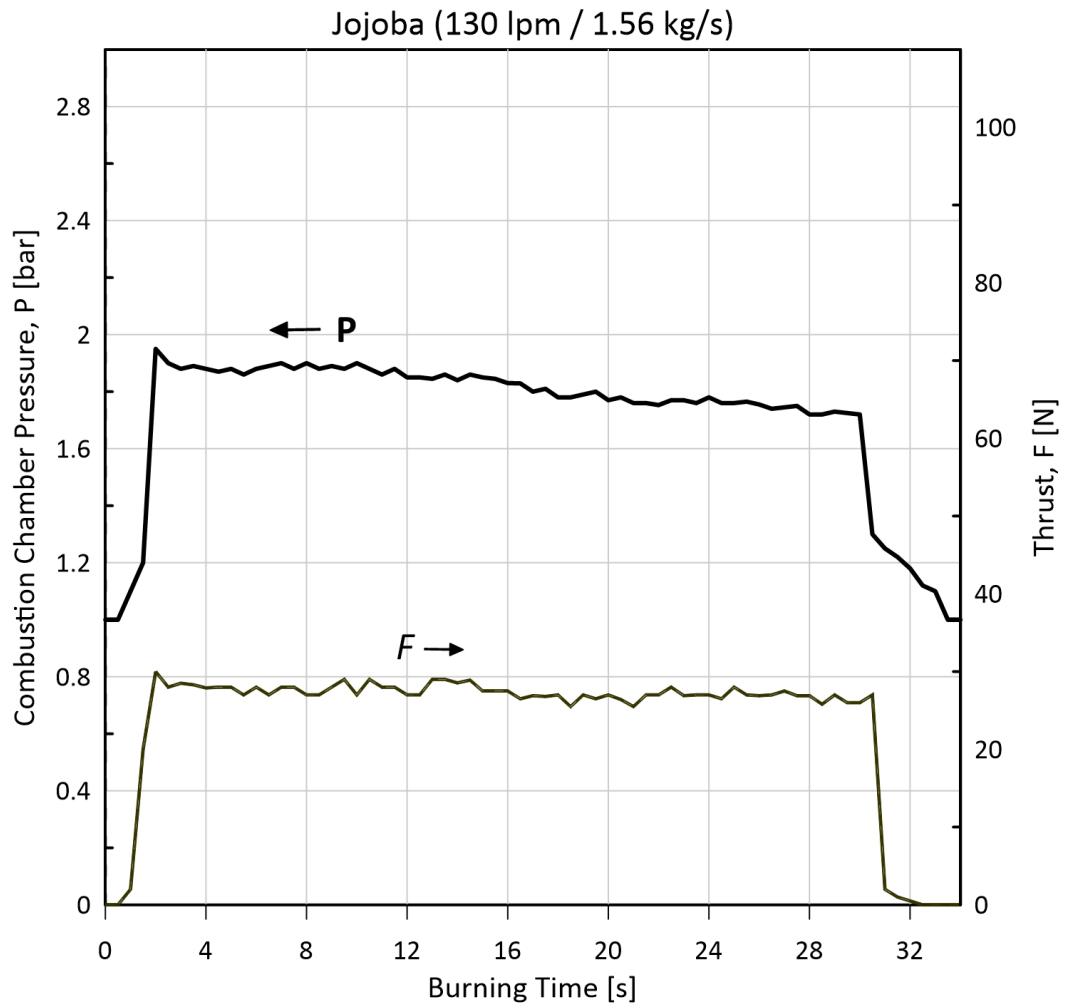


Figure 30: Thrust and pressure profiles for the tested Jojoba Solid waste propellant with bar and Newton units respectively. The Oxidizer volume flow rate applied around 130 lpm (~ 1.56 kg/s) in 30 second burning time.

Unlike previous tests for Date Stone and Jojoba, this run showed no noticeable difference in thrust profile compared to Jojoba 110 lpm in terms of stability. The combustion pressure profile recorded a peak of 1.9 bar higher with a negative slope toward the end of the run.

Figures 32, 33 and 34 show pressure and thrust profiles for PW-based propellant combustion at three oxygen volume flow rates of 80, 110 and 130 lpm, respectively.

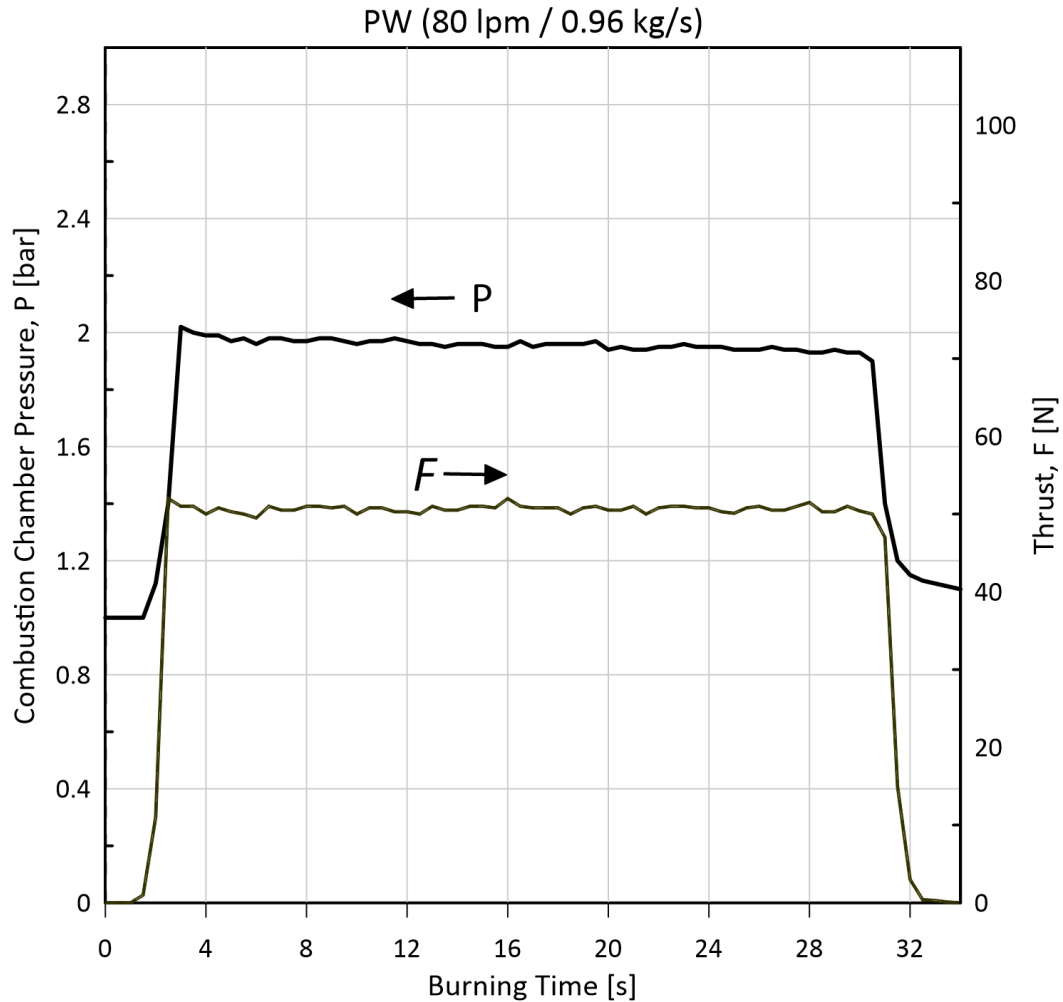


Figure 31: Thrust and pressure profiles for the tested Paraffin Wax propellant with bar and Newton units respectively. The Oxidizer volume flow rate applied around 80 lpm (~ 0.96 kg/s) in 30 second burning time.

With a thrust exceeding 50 N and a pressure value of around 1.9 bar throughout the burning time, PW-based fuel performance is significantly higher than biomass fuels in terms of combustion pressure and thrust profiles considering the same volume flow rate condition. However, the thrust profile showed similar fluctuations as in previous tests. Furthermore, the combustion pressure profile showed less negative pressure

slope compared to other fuels and more stability while increasing the oxidizer volume flow rate as shown in Figure 33.

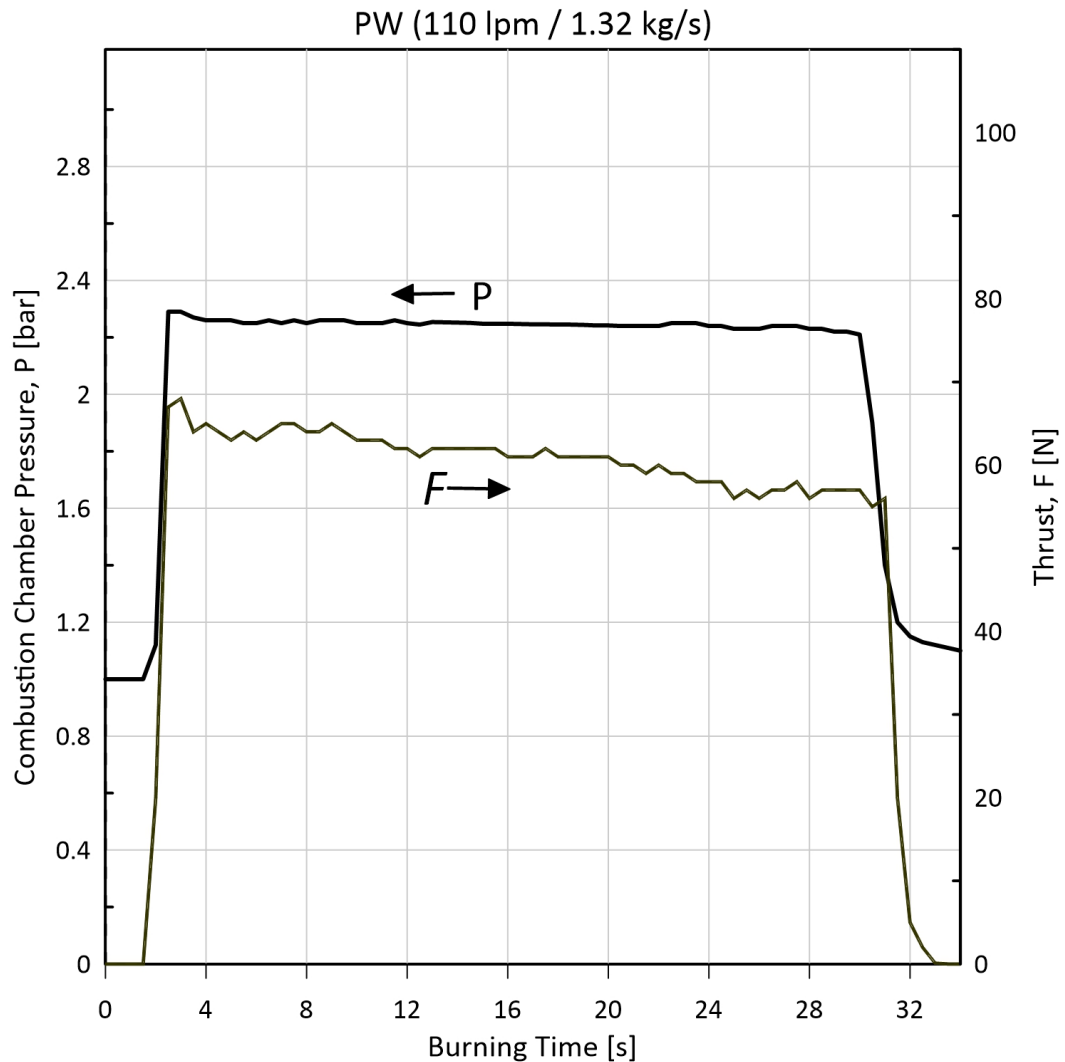


Figure 32: Thrust and pressure profiles for the tested Paraffin Wax propellant with bar and Newton units respectively. The Oxidizer volume flow rate applied around 110 lpm (~ 1.32 kg/s) in 30 second burning time.

With a 110 lpm oxygen volume flow rate, a higher-pressure value of 2.25 bar was recorded and almost remained constant during the burning time. Meanwhile, the thrust profile started with 69 N and was followed by a fluctuating decline till the end of the run. grater fluctuation and a consistent drop during the experiment from 69 N to 60 N. The combustion pressure showed exceptional stability at 2.3 bar during the burning

time, which suggests that better stability exists with PW-based compared to biomass fuels.

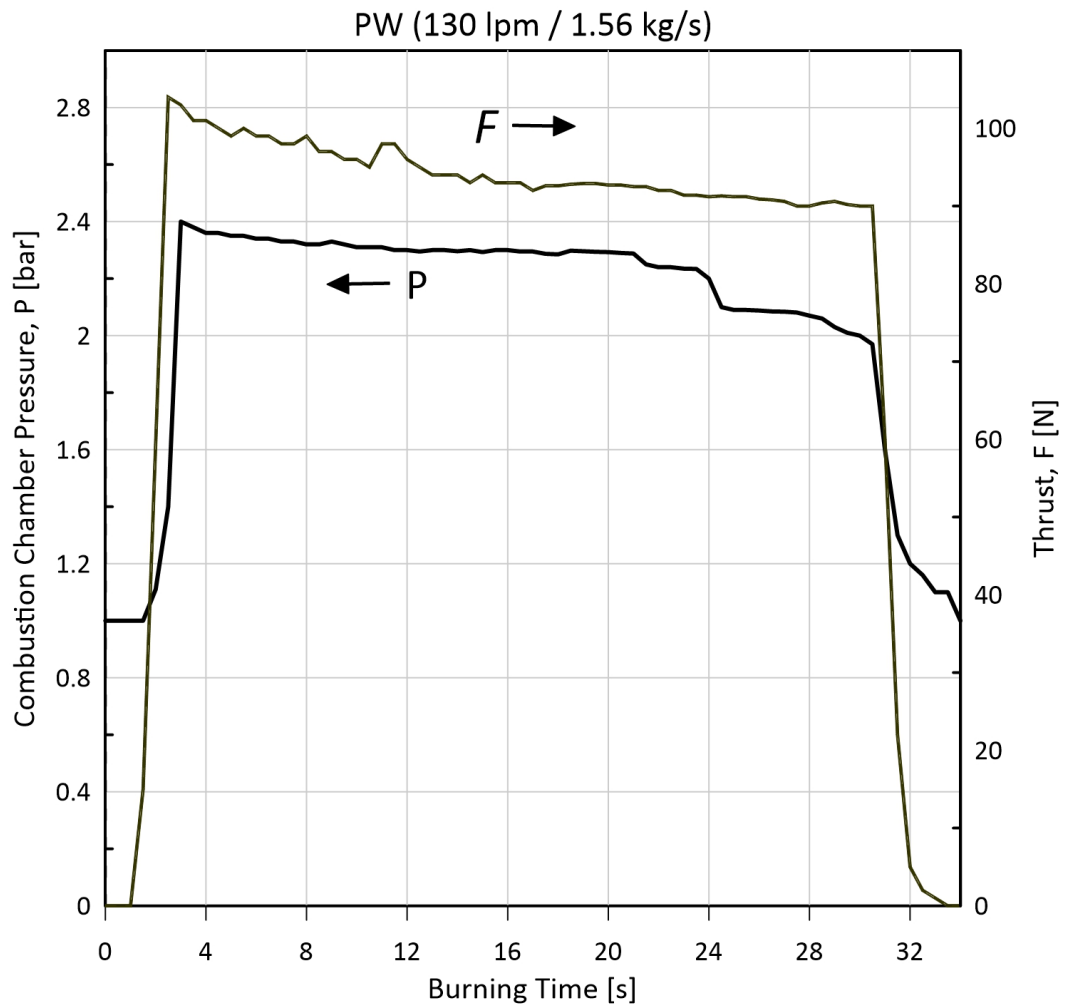


Figure 33: Thrust and pressure profiles for the tested Paraffin Wax propellant with bar and Newton units respectively. The Oxidizer volume flow rate applied around 130 lpm (~ 1.56 kg/s) in 30 second burning time.

The combustion pressure showed a significant change in performance by applying an oxygen volume flow rate of 130 lpm. Except for the higher pressure recorded, the pressure showed a significant decline during the test and considerable fluctuation in the first 15 seconds of burning time. Moreover, the pressure showed a dramatic drop

at the second 21 and even more at the second 24, as shown in Figure 34. The thrust profile showed more fluctuation while the oxidizer flow rate increased.

For better understanding and clearer comparison, pressure profiles were merged into one graph to show the variation in pressure among tested fuels. Figure 35 shows the pressure profile for all tested fuels based on an oxygen volume flow rate of 80 lpm, while Figures 36 and 37 show the pressure profile at 110 and 130 lpm, respectively.

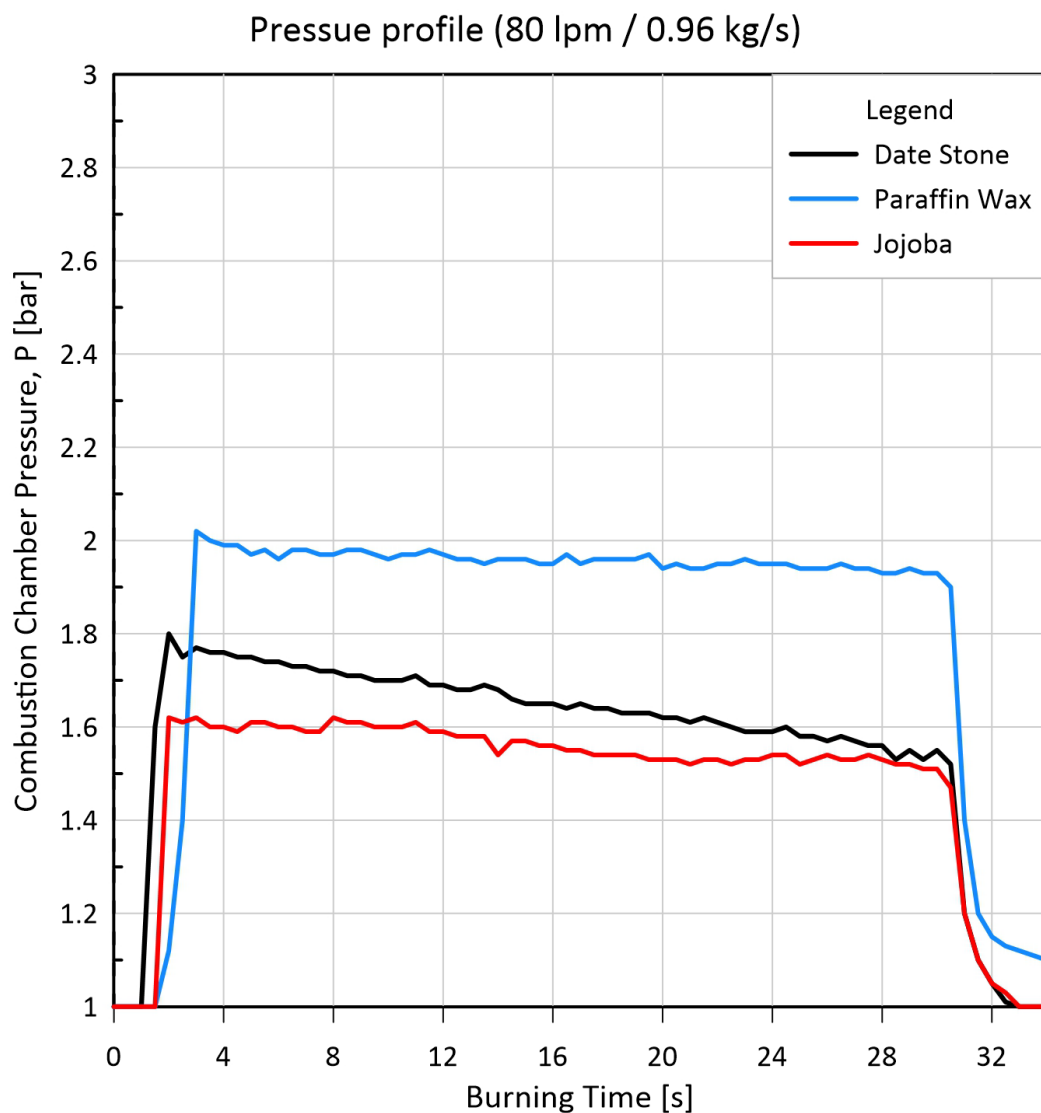


Figure 34: Pressure profile for all tested propellants with oxidizer volume flow rate of 80 lpm (~ 0.96 kg/s).

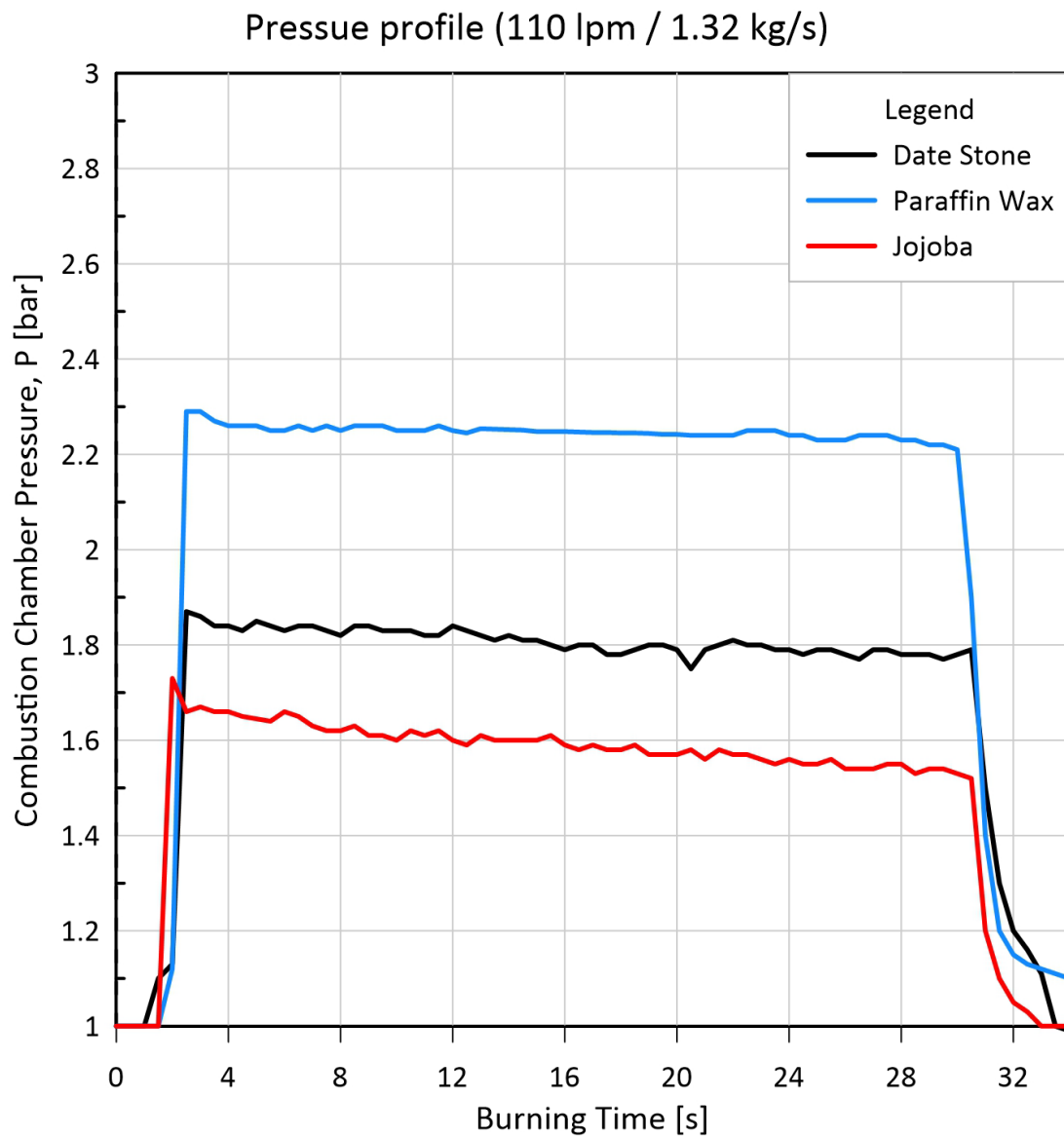


Figure 35: Pressure profile for all tested propellants with oxidizer volume flow rate of 110 lpm (~ 1.32 kg/s).

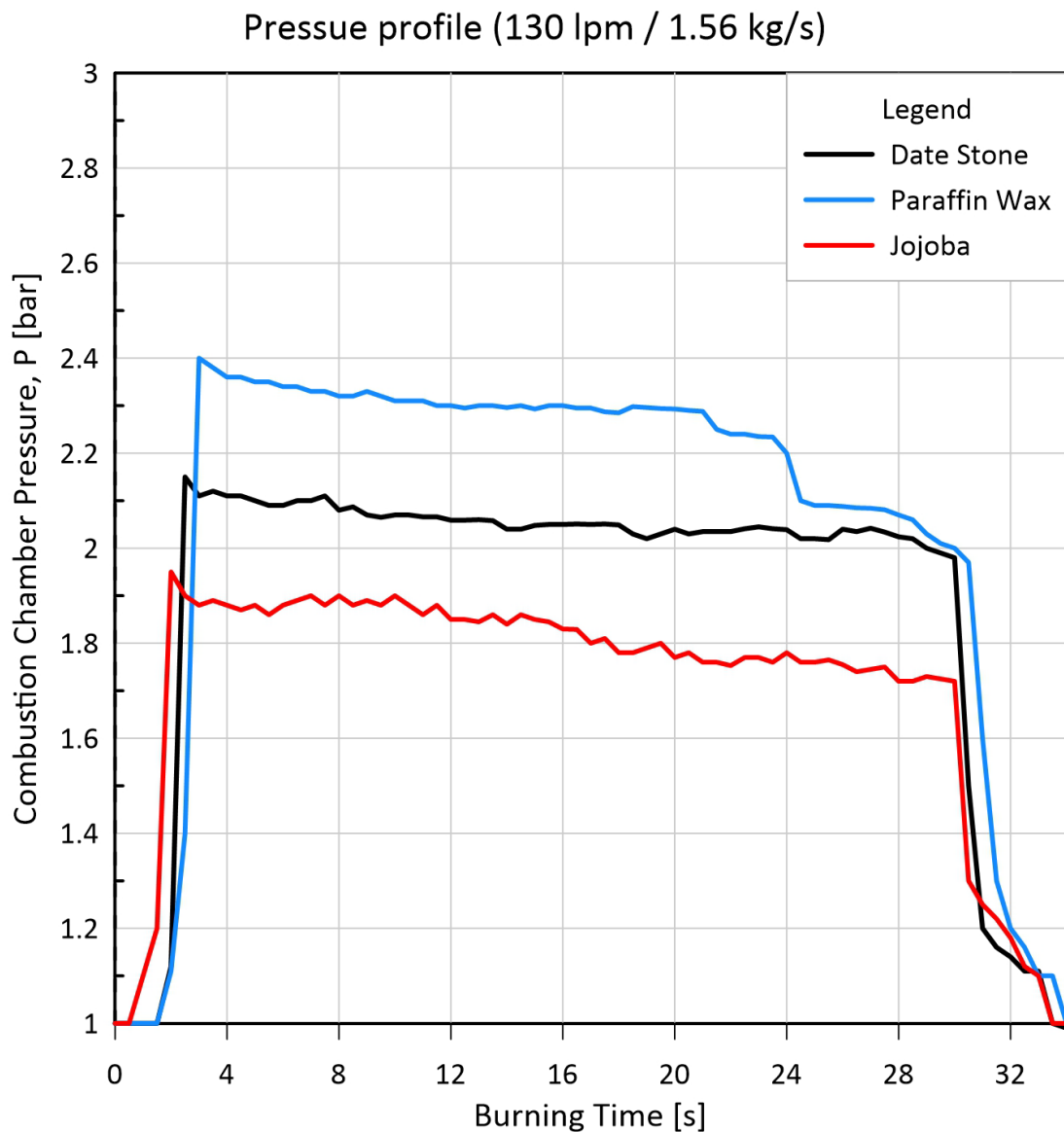


Figure 36: Pressure profile for all tested propellants with an oxidizer volume flow rate of 130 lpm (~ 1.56 kg/s).

Based on the performance of combustion chamber pressure for all proposed fuels, we can conclude that the gap between PW-based pressure and other biomass propellants is decreasing while increasing the oxidizer mass flow rate. However, PW-based chamber pressure tends to be more stable with lower oxygen mass flow rates. In general, it is obvious that no choking took place during the firing which is due to low

pressure ratio between the pressure inside combustion chamber and nozzle exit pressure which require a ratio of 10-30 bar [55] for similar rocket size.

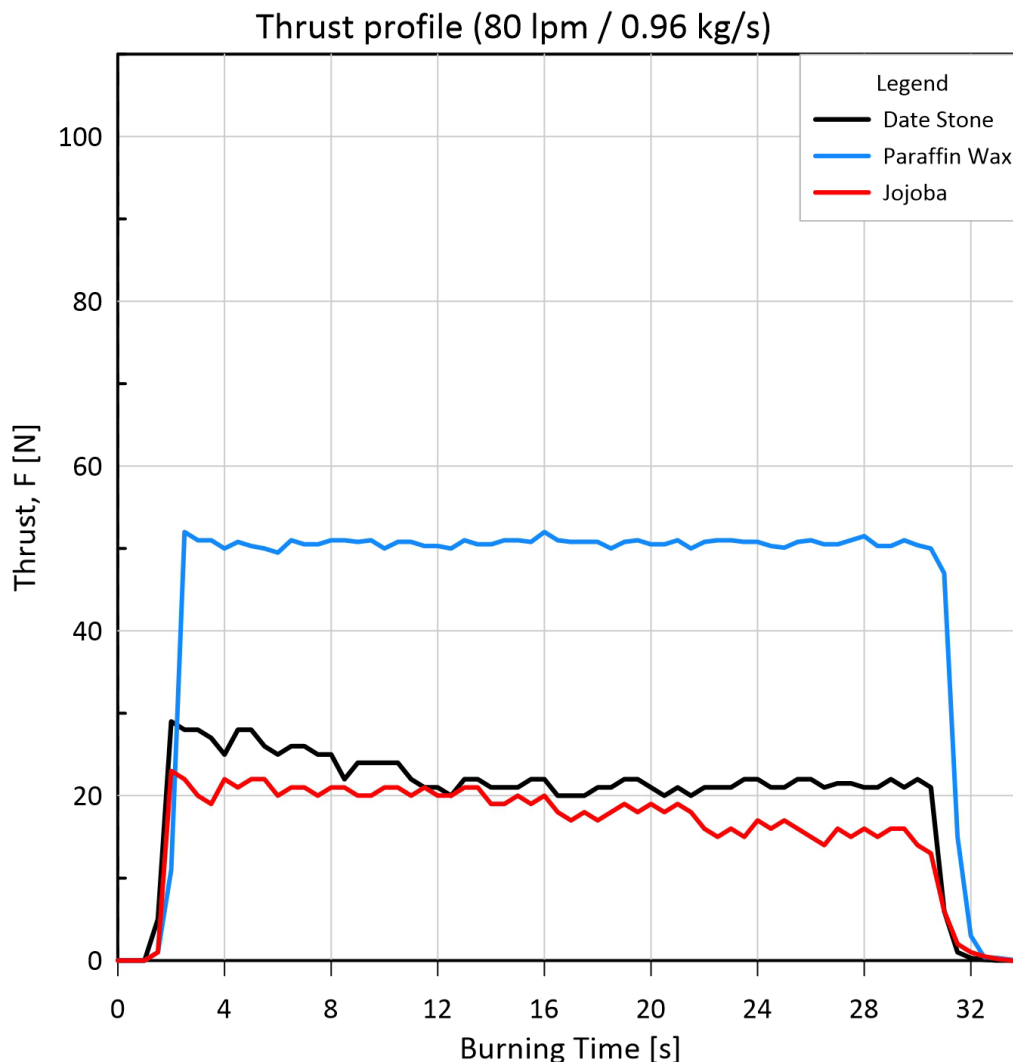


Figure 37: Thrust profile for all tested propellants with oxidizer volume flow rate of 80 lpm (~ 0.96 kg/s).

Similarly, thrust profiles were merged into one graph to show the variation in thrust among tested fuels. Figure 38 shows the pressure profiles for all tested propellants based on a volume flow rate of 80 lpm, while Figure 39 and Figure 40 show the pressure profiles at 110 and 130 lpm, respectively.

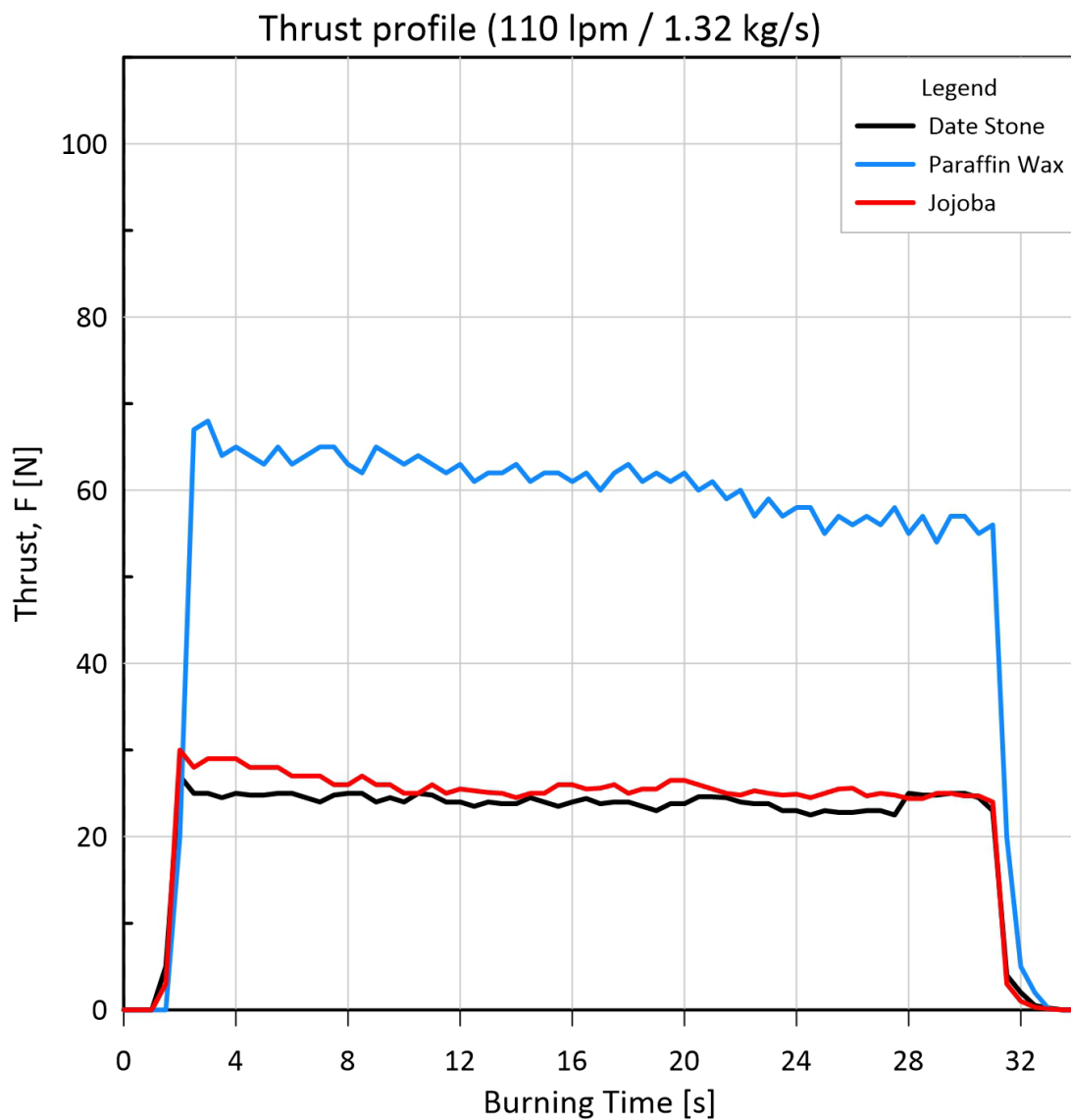


Figure 38: Thrust profile for all tested propellants with oxidizer volume flow rate of 110 lpm (~ 1.32 kg/s).

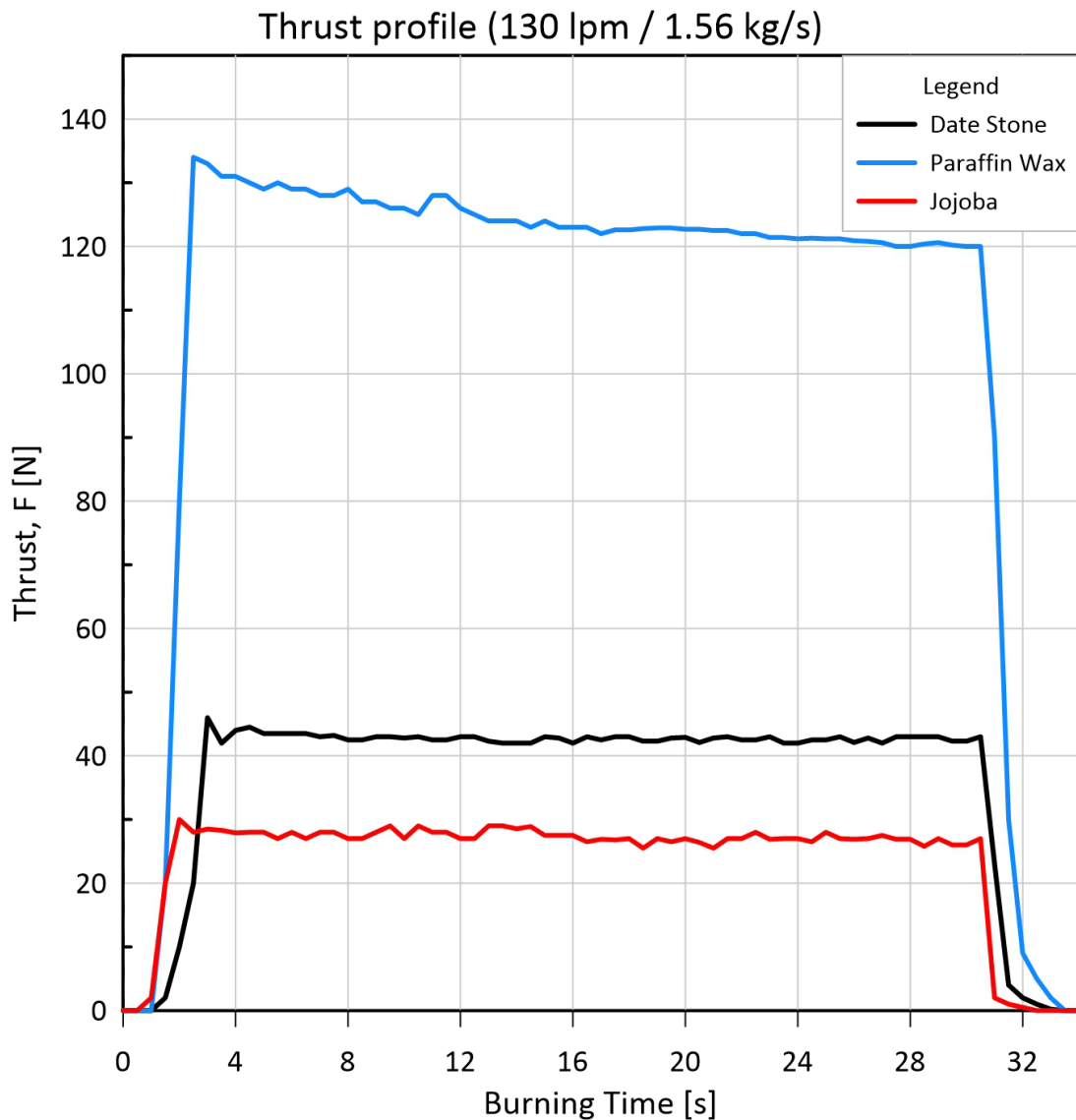


Figure 39: Pressure profile for all tested propellants with oxidizer volume flow rate of 130 lpm (~ 1.56 kg/s).

Based on the thrust profiles for all proposed propellants under different oxidizer volume flow rates, PW-based fuel showed higher thrust under all volume flow rate conditions. Moreover, the gap between the PW-based propellant's thrust was shrinking with higher oxidizer volume flow rates. On the other hand, for lower mass flow rates, Date Stone and Jojoba showed similar performance. However, under an oxidizer volume flow rate of 130 lpm, Date Stone recorded a considerably higher thrust force compared to jojoba. It is also worth mentioning that under a volume flow rate of 80

lpm, PW-based propellant showed more thrust stability while the opposite behavior took place with higher volume flow rates (i. e., 110 and 130 lpm).

4.2.2 Nominal Thrust, and Impulse Measurements

Total impulse for test fuels in the integral of thrust curves presented earlier in the operation time frame, which is 30 seconds. The integral for the experimental data obtained can be attained by dividing the trend into small segments of width multiplied by the average value within each segment. The segments are divided equally to have a constant through the testing period, resulting in segments for the total testing period.

This yields the following equation:

$$I_t = \sum_1^n \Delta t \cdot F_n \quad (4.4)$$

where n is the number of segments with a maximum value of 60. Meanwhile, specific impulse represents the total impulse divided by the fuel mass prior to the firing test as follows:

$$I_s = \frac{I_t}{m} \quad (4.2)$$

Where I_s stands for the specific impulse and stands for fuel mass. Furthermore, using total impulse value, the nominal impulse is calculated by dividing the total impulse over the testing time as follow:

$$F_{nom} = \frac{I_t}{30} \quad (4.3)$$

Starting from the case of an 80 lpm oxidizer flow rate for all tested fuels, total impulse is the total area under each thrust force curve as shown in Figure 41.

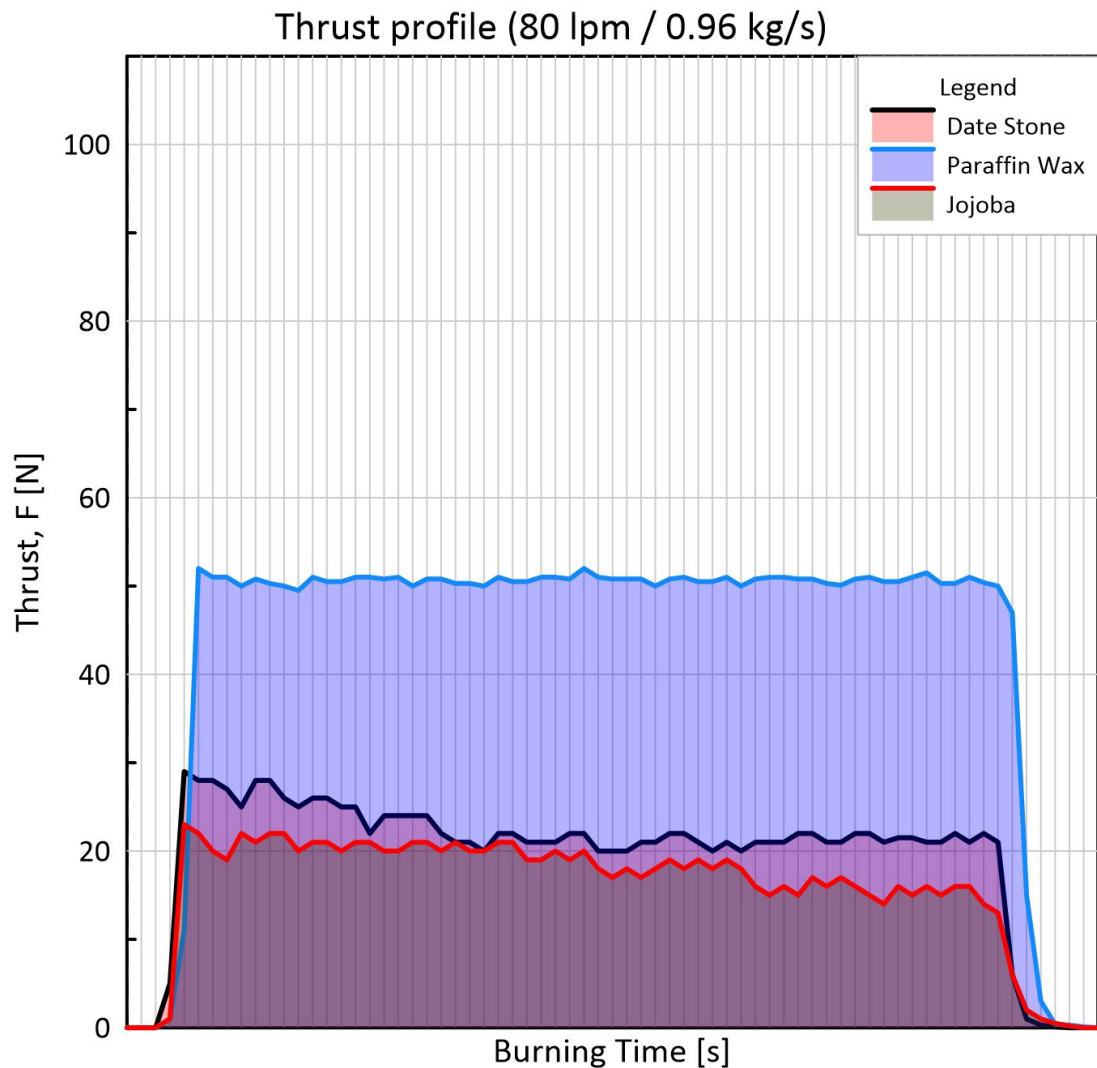


Figure 40: Total impulse for all fuels under GOX of 80 lpm (0.96 kg/s).

The nominal thrust was calculated for all fuels where the highest was PW-based fuel with 49.44 and followed by Date Stone with 22.07 and the lowest value of 18.08 for Jojoba fuels. By using Equation 4.1 of total impulse for PW-based fuel data, the calculated total impulse is 1483. Meanwhile, Date Stone and Jojoba recorded 662.2 and 542.4, respectively. Using Equation 4.2, the specific impulse of PW-based reached

0.674, while Date Stone and Jojoba fuels recorded 0.331, and 0.262, respectively.

Table 8 summarizes the results for this case.

Table 8: Thrust nominal, total impulse, and specific impulse for all fuels with oxidizer flow rate of 80 lpm.

Fuel	I_t	I_s	F_{nom}
PW-Based	1483	0.674	49.44
Date Stone	662.2	0.331	22.07
Jojoba	542.4	0.262	18.08

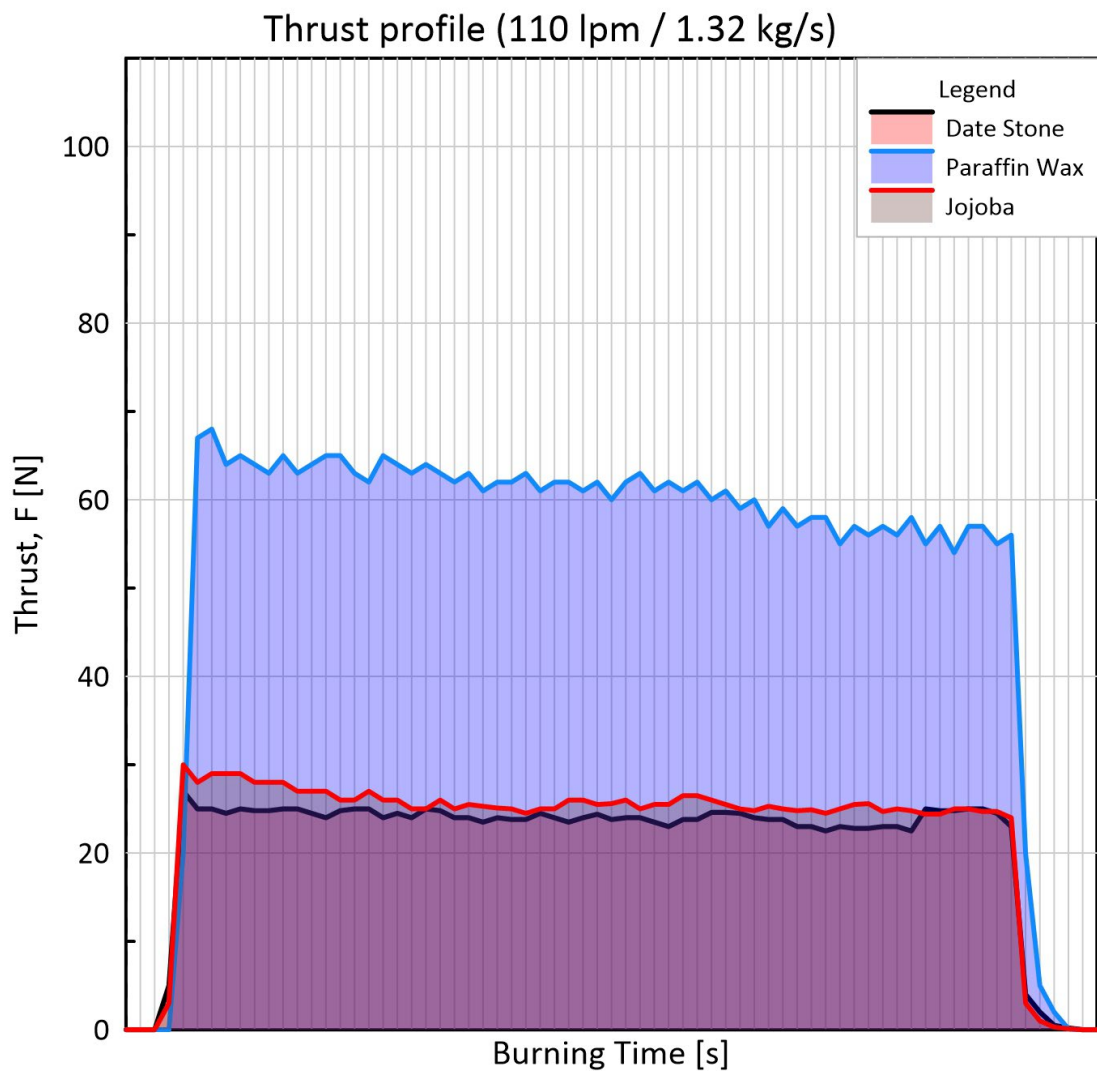


Figure 41: Total impulse for all fuels under GOX of 110 lpm (1.32 kg/s).

Like previous case, total impulse is the total area under each thrust force curve as shown in Figure 42. The same calculation procedure applied for 110 lpm oxidizer rate case and the results are shown in Table 9.

Table 9: Nominal thrust, total impulse and specific impulse for all fuels with oxidizer flow rate of 110 lpm.

Fuel	I_t	I_s	F_{nom}
PW-Based	1788	0.813	59.59
Date Stone	717.9	0.359	23.93
Jojoba	765.8	0.37	25.53

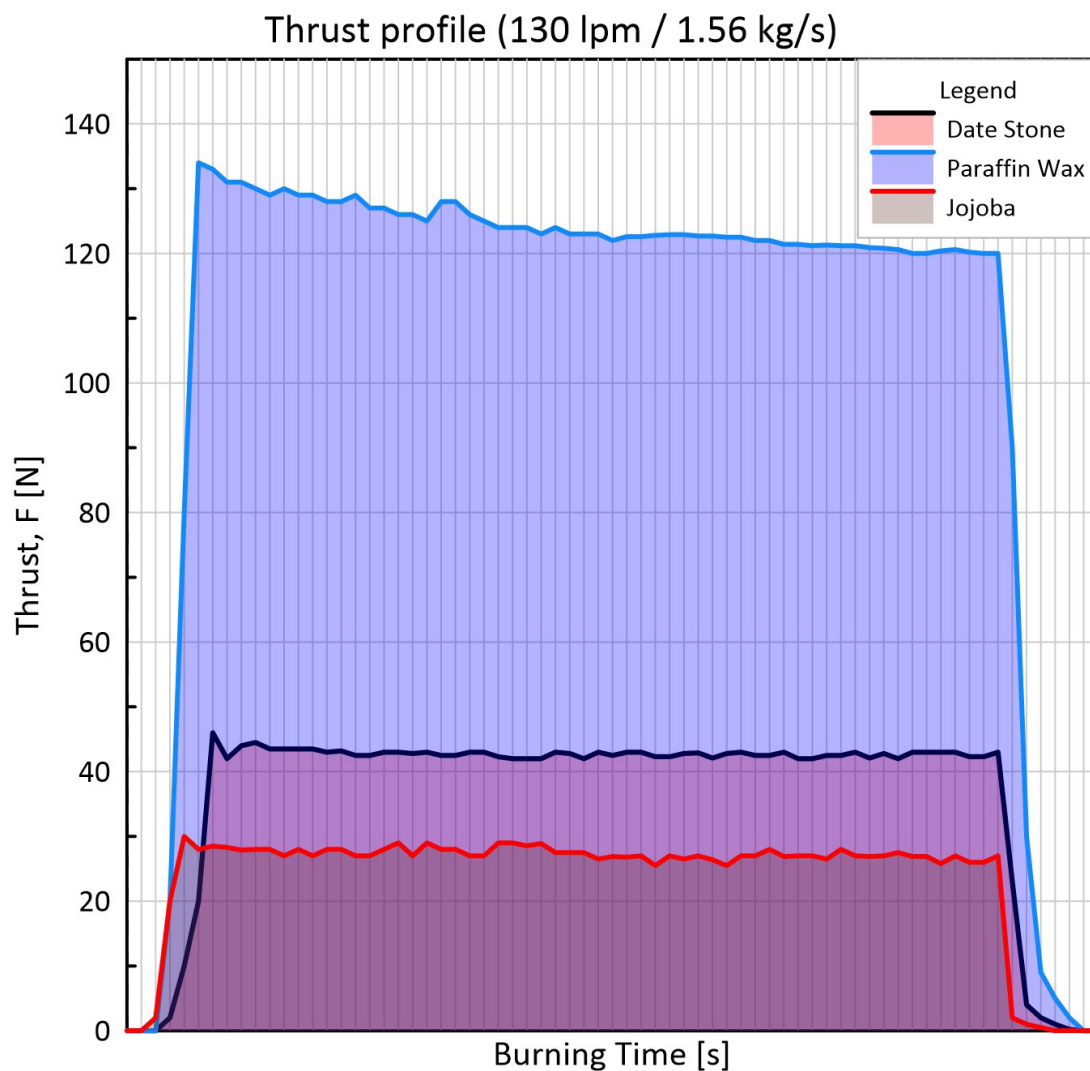


Figure 42: Total impulse for all fuels under GOX of 130 lpm (1.56 kg/s).

In the case of 130 lpm, total impulse is the total area under each thrust force curve as shown in Figure 43. The nominal thrust, total impulse and specific impulse are summarized in Table 10.

Table 10: Nominal thrust, total impulse, and specific impulse for all fuels with oxidizer flow rate of 130 lpm.

Fuel	I_t	I_s	F_{nom}
PW-Based	2772	1.26	92.39
Date Stone	1230	0.615	40.98
Jojoba	806.8	0.39	26.89

Based on that, it's clear that PW-based fuel recorded better total impulse, specific impulse, and nominal thrust compared to biomass fuels through all oxidizer flow rate conditions. For the same parameter, Date Stone showed better performance than Jojoba. However, it's clearly that biomass fuels showed relatively similar performance for 80 lpm and 130 lpm in favor of Date Stone, while the difference was big between them for the 130 lpm flow rate shown in Table 10.

4.2.3 Oxidizer-Fuel Ratio

For each run, the mass of the propellant grain was measured before and after burning to calculate the mass loss during the test for the purpose of calculating the Mass to Fuel (O/F) ratio. The O/F ratios were calculated by dividing the oxidizer's mass (m_{GOX}) injected during the testing time by the fuel's mass loss (m_{fuel})

$$O/F = \frac{m_{GOX}}{m_{fuel}} \quad (4.3)$$

Where m_{fuel} is the difference between initial propellant mass (m_i) and final propellant mass (m_f) as shown in Equation 2.

$$m_{fuel} = m_i - m_f \quad (4.4)$$

m_{GOX} stands for the whole amount of oxidizer mass entered the combustion chamber during the burning process which can be calculated by multiplying the mass flow rate per second by the total testing time, which is 30 seconds, as shown in Equation 3.

$$m_{GOX} = \dot{m} \times 30 \quad (4.5)$$

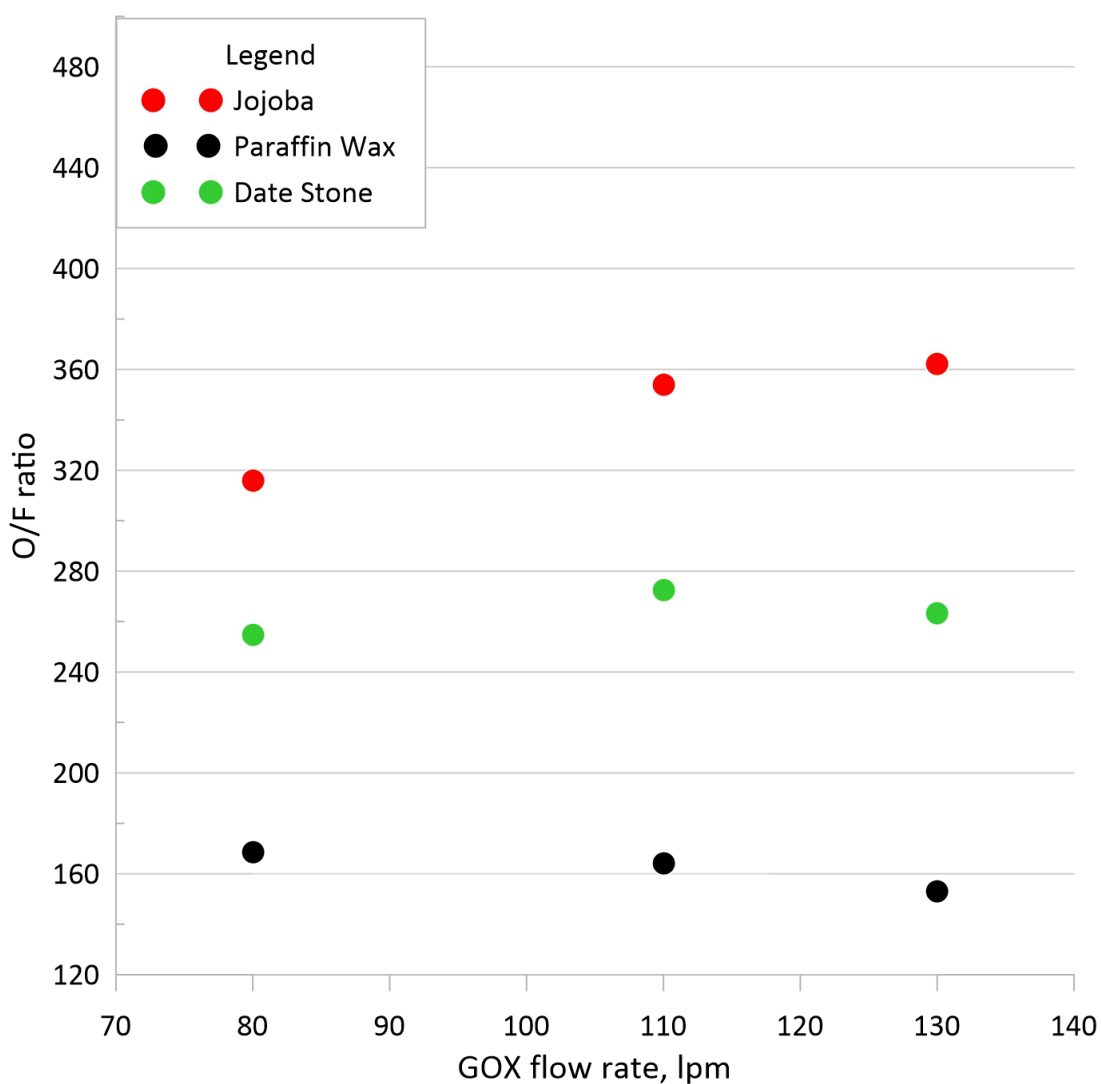


Figure 43: O/F ratio for all runs.

Figure 44 shows the O/F ratios for each run under a specific oxidizer mass flow rate. The O/F ratios for PW-based propellant were the lowest in comparison with other biomass fuels. However, O/F ratios for Date Stone were significantly lower than for Jojoba. PW-based fuel recorded the highest O/F ratio of 170 at the lowest volume flow rate, while Jojoba recorded the highest value of 362 at the maximum volume flow rate implemented. However, the Date Stone O/F ratio reached a peak of 275 at 110 lpm before decreasing to almost 265. This finding is reasonable considering that Date Stone contained almost twice the amount of oxygen content compared to Jojoba. Not only that, but also, it matches with the combustion characteristics revealed in the TGA test showing that Date Stone contains a higher amount of volatile matter, fixed carbon, and less moisture compared to Jojoba grains, so more complete combustion is expected. However, O/F ratio is much higher than normal O/F ratio of HTPB and PW fuels which is around 2 [56].

4.2 Combustion Temperature Profile for Different Fuels

By mounting the thermocouple inside the combustion chamber near the nozzle, temperature profiles were measured for each fuel under different oxidizer mass flow rates.

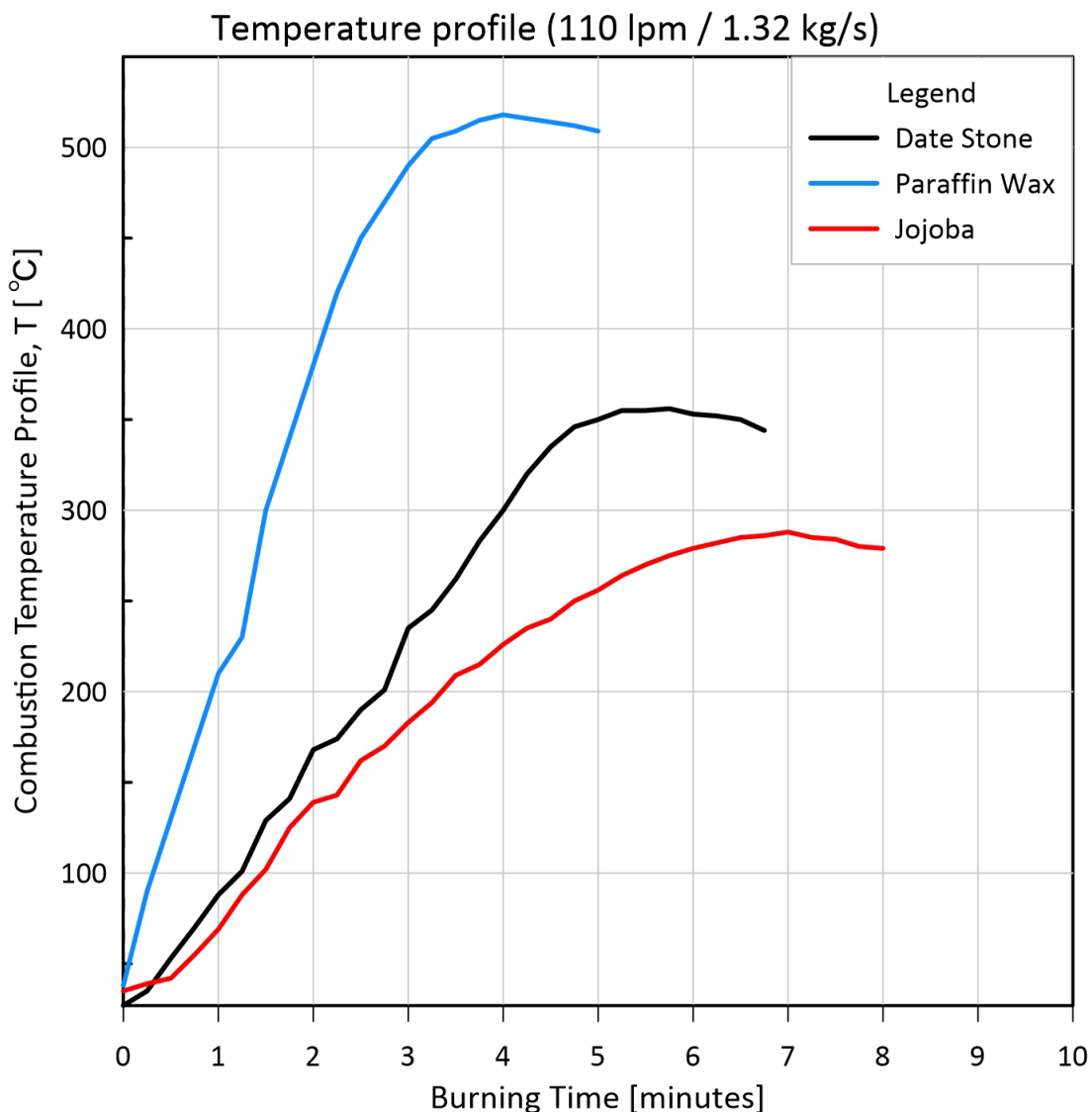


Figure 44: Temperature profile for tested propellants with oxidizer volume flow rate of 110 lpm (~ 1.32 kg/s).

Figure 45 illustrates the chamber temperature profiles combined into one plot for comparison. The peak for each trend represents the end of grain burning, so no flame is generated due to a lack of combustion reaction. It's obvious that PW-based fuel had a significantly higher temperature inside the combustion chamber than other biomass fuels. However, the combustion of biomass fuels lasted much longer than that of PW-based fuel, where PW-based fuel ended in 4 minutes while Date Stone and Jojoba

lasted for 5.5 and 7 minutes, respectively. A steady temperature gradient was the dominant feature during burning time for all tested fuels to reach a peak of 520°C, 350°C, and 281°C for PW-based, Date Stone, and Jojoba, respectively. In general, the higher the temperature, the less burn time there is. Based on that, we can conclude that this result supports the TGA results from Section 4.1, which showed better combustion characteristics for Date Stone compared to Jojoba fuel. This result is also consistent with the fact that paraffin wax is more reactive, considering its higher carbon content. The next section will discuss the length of the flame generated by each fuel in the round 1 firings.

4.4 Flame Visualization

In addition to previous comparing parameters, the length of flame for each run was recorded using a smartphone camera, where photos were taken after 5 seconds of burning. The flame length was measured using online scaling software where the nozzle length in the photo was used as a reference to calculate the length of the flame as shown in Figure 46.



Figure 45: Representation of measuring methodology for the PW flame length at an oxidizer volume flow rate of 130 lpm. Where 6.49 equals 100.4 cm.

For example, the actual length of the nozzle is 154.58 mm, which will take the reference length of 1 in the photo. Based on that, the reference length of the flame is 6.49 which means it's 6.49, times the nozzle length (i.e $154.85 \text{ mm} \times 6.49 = 1005 \text{ mm} \approx 100.4 \text{ cm}$). Similarly, the same procedure was repeated for all runs.



Figure 46: Flame length of Date Stone propellant at 130 lpm where 2.7 equals 41.8 cm.

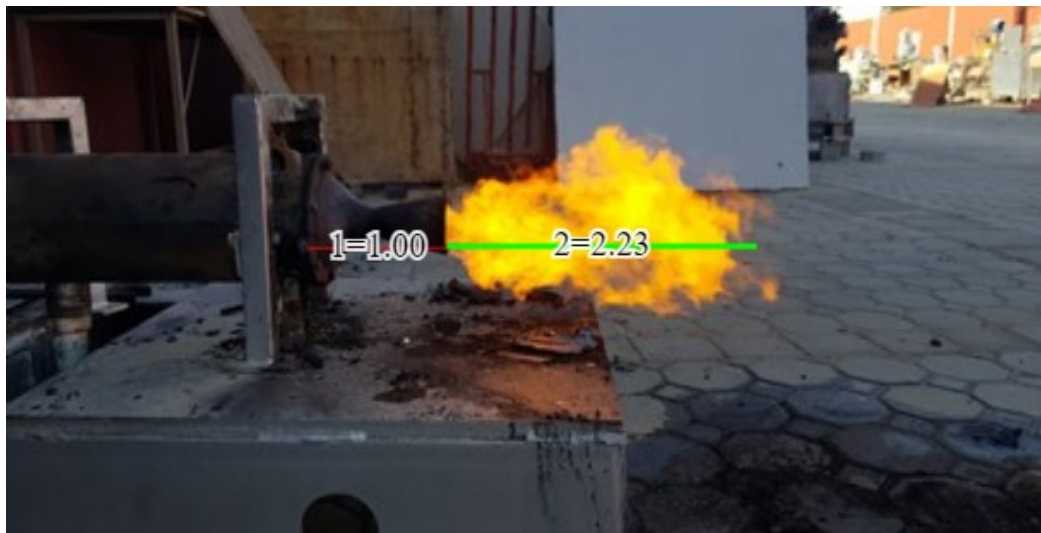


Figure 47: Flame length of Jojoba propellant at 110 lpm where 2.23 equals 34.5 cm.

Figures 47 and 48 show examples of Date Stone and Jojoba flames with different oxygen mass flow rates. The flame lengths for all propellants at different oxygen mass flow rate conditions are presented for comparison in Figure 49.

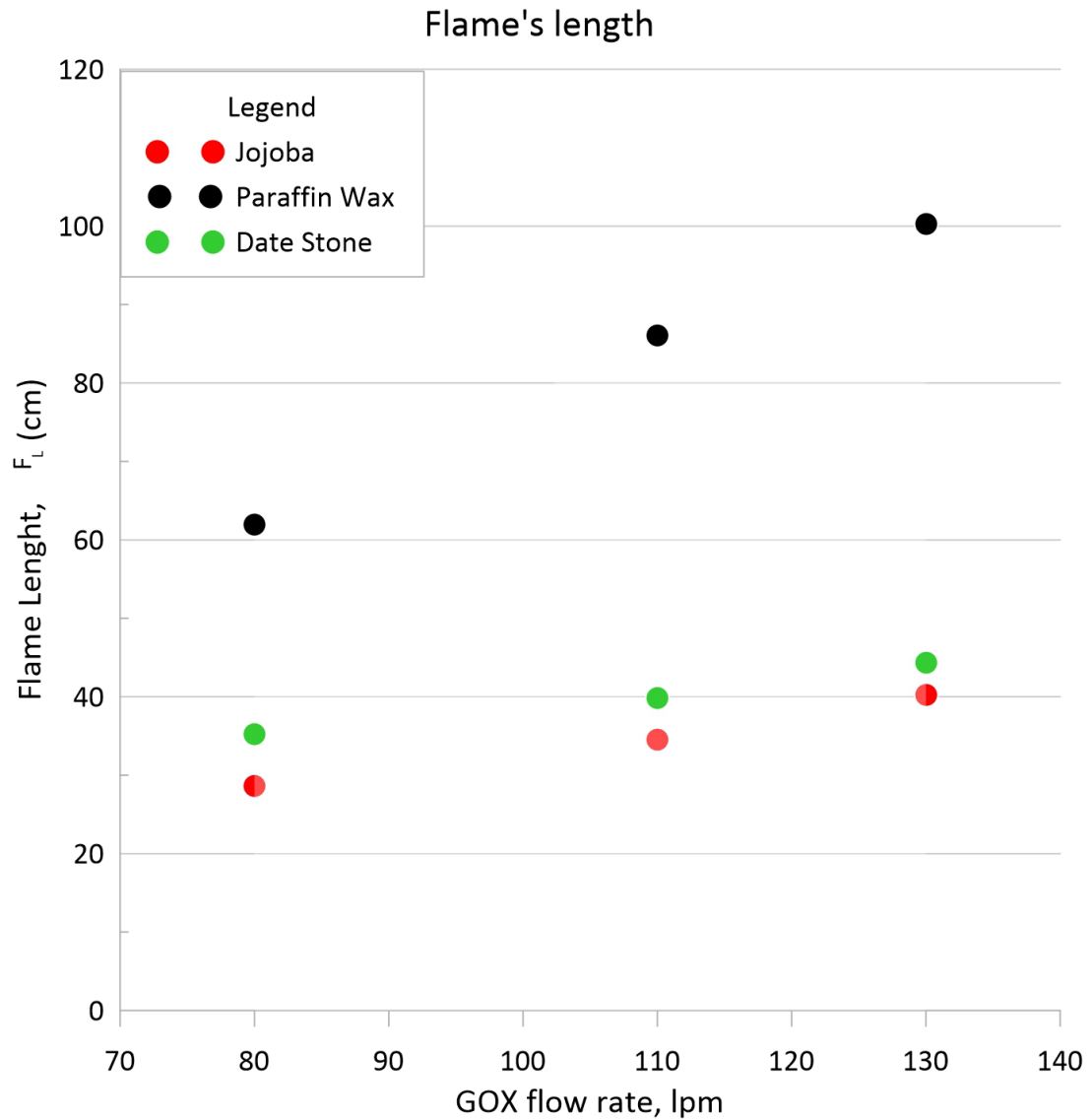


Figure 48: Flame length representation with variant oxidizer volume flow rate for all tested propellants.

As expected, all fuels followed a similar trend where the flame length increased with higher oxygen volume flow rate. PW-based fuel recorded the highest flame length under all volume flow rate conditions compared to biomass fuels. The maximum flame

length for PW-based fuel reached almost 100 cm at 130 lpm and the lowest length was 62 cm at 80 lpm. Date Stone and Jojoba fuels had similar and consistent performance where they had almost the same increasing slope. However, under all oxygen volume flow rates, Date Stone recorded slightly higher values. The maximum flame length for Date Stone fuel was 46 cm at 130 lpm while the maximum flame length for Date Stone fuel was 41 cm at the same flow rate condition. We can conclude that the flame of PW-based propellant is significantly longer than the others', while Date Stone and Jojoba fuels have relatively similar lengths with a small advantage in favor of Date Stone.

4.5 Error Analysis

Like in any experimental investigation, an expected measurement error would create a variation while repeating the runs even with the same proposed conditions. There are many factors that could be considered in the current study, such as friction between the outer surface of the combustion chamber and the bearing wheels. However, a lubrication procedure took place before each run to ensure smooth contact between the surfaces. Moreover, the inaccuracy error from the measuring devices, such as force meters, pressure transducers, and temperature thermocouples, is expected to contribute to experimental errors. The leakage of pressure was a serious challenge, especially for flanges from both sides, taking into consideration the high temperature that can melt the rubber installed between flanges to prevent leakage. However, an anti-heat rubber was used to minimize the possibility of burning. There are random error and systematic error that is taking place in experimental work. The random error is the unpredicted error that is affected by many factors we can't control effectively especially environmental condition changes in term of temperature and humidity. On

the other hand, the systematic error could be calculated from repeated runs for experimental data.

4.5.1 Systematic Error

The systematic error for measured and calculated data could be found starting by calculating the average value as shown in the following equation:

$$Avg = \frac{\sum_1^{60} x}{30 \times 2} \quad (4.4)$$

Where x is the measured value and the testing time was 30 seconds, and the values were measured each 0.5 second. The result value is the average Pressure/Thrust force for each fuel during the testing period. After calculating average value, the deviation was calculated as follows:

$$Dev = |Avg - x| \quad (4.5)$$

Once the deviation value is calculated, the average deviation Avg_D to be calculated as shown in the following equation:

$$Avg_D = \frac{\sum_1^{60} Dev}{30 \times 2} \quad (4.6)$$

This procedure was repeated for all fuels with all oxidizer flow rate conditions and summarized in Table 11.

Table 11: Average, Average Deviation and Error Percentage values for all tested fuels for chamber pressure and trust force measured values.

	Fuel (GOX), lpm	Avg	Avg Div	Error %
Pressure	Date Sone (80)	1.61	0.09	5.81
	Date Sone (110)	1.75	0.10	5.69
	Date Sone (130)	1.96	0.17	8.87
	Jojoba (80)	1.53	0.06	4.26
	Jojoba (110)	1.55	0.08	5.18
	Jojoba (130)	1.76	0.11	6.44
	Paraffin Wax (80)	1.87	0.15	7.99
	Paraffin Wax (110)	2.14	0.19	9.01
	Paraffin Wax (130)	2.14	0.23	10.7
Thrust	Date Sone (80)	22.0	2.28	10.39
	Date Sone (110)	23.80	1.03	4.33
	Date Sone (130)	40.90	3.55	8.68
	Jojoba (80)	18.03	2.56	14.22
	Jojoba (110)	25.45	1.31	5.13
	Jojoba (130)	26.52	1.80	6.79
	Paraffin Wax (80)	49.36	2.50	5.07
	Paraffin Wax (110)	59.47	4.36	7.33
	Paraffin Wax (130)	92.01	5.17	5.62

Based on data presented in above table, the maximum error percentage in pressure measurement is 10.7 associated with PW-based fuel firing under oxidizer flow rate of 130 lpm. on the other hand, the lowest was 4.26 for Jojoba biomass fuel under oxidizer flow rate of 80 lpm. it's clearly obvious that the error percentage tend to increase with increasing oxidizer flow rate. Furthermore, Biomass fuel recorded lower error percentages compared to PW-based fuel in all oxidizer flow rate conditions. For thrust error analysis, the same conclusion can't be achieved due to variation in error percentages among all tested fuel. The maximum error for thrust data appeared in Jojoba fuel testing under 80 lpm oxidizer flow rate with 14.22, while the minimum value was 4.33 for Date Stone at 110 lpm oxidizer flow rate condition.

Systematic error could be calculated also from the error margin and accuracy of measuring devices using in the experiment. The force meter and pressure transducer have a limited reading capacity were the relative error percentage for each can be calculated by dividing the Minimum Scale Reading can be read by the minimum value measured as shown in the following equations:

$$RE = \frac{MRN}{MV} \times 100 \quad (4.7)$$

where're stands for the relative error, MSR is Minimum Scale Reading and MMV is the Minimum Measured Value. The calculation results are shone in Table 12 below.

Table 12: Relative error calculated for measuring devices.

Measuring device	MRN	MV	Unit	RE %
Force Meter	0. 1	13.0	N	0.8
Pressure transducer	0.01	1.47	Bar	0.7

4.5.2 Random Error

To study the random error in this research, a repeated tests were conducted using the same amount of fuel and same condition in terms of oxidizer flow rate for PW-based fuel at 80 lpm oxidizer flow rate and Date Stone biomass fuel at 110 lpm oxidizer flow rate where the test was repeated three times for both cases as shown in Figure 50 and 51. The consistency of performance with repeated runs illustrated the small margin of experimental error in this study and repeatedly showed the direct relationship between the chamber pressure profile with thrust force. In other words, the higher the pressure achieved, the higher the thrust force delivered.

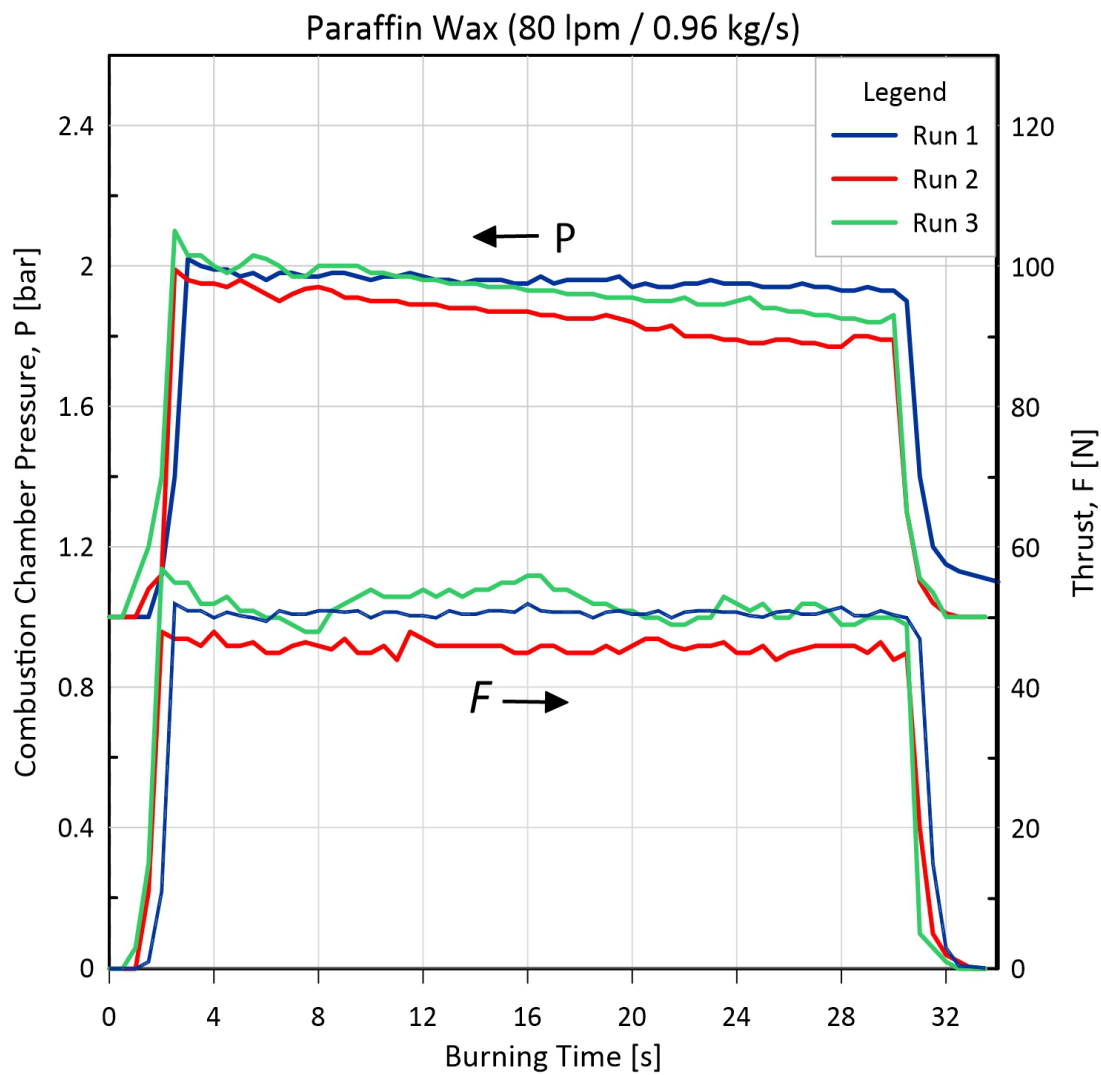


Figure 49: Three runs for PW-based fuel at a volume flow rate of 80 lpm (0.96 kg/s).

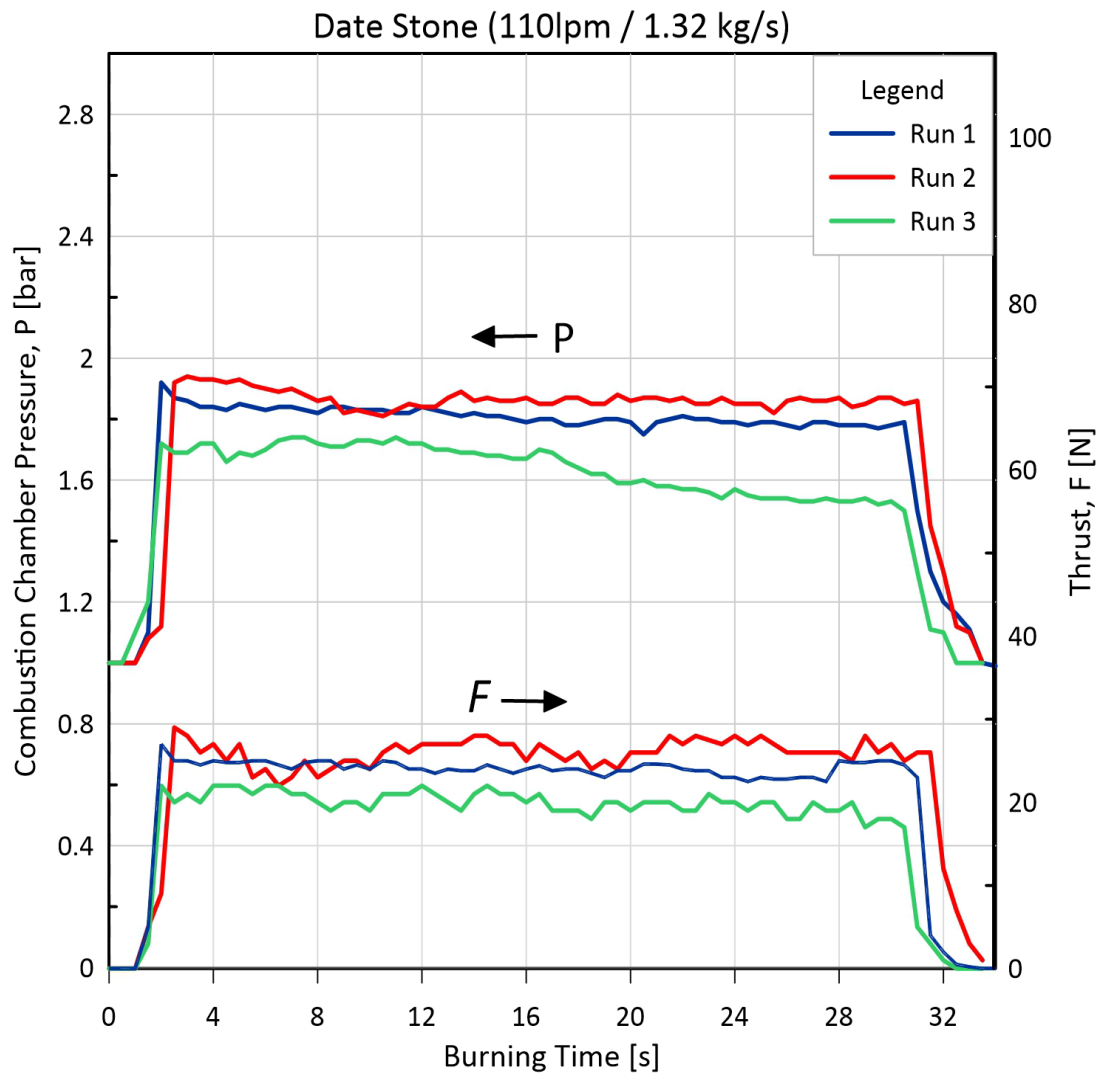


Figure 50: Three runs for Date Stone fuel at volume flow rate of 110 lpm (1.32 kg/s).

Based on the results shown in the diagrams we can calculate the random error by finding the largest difference between two values at the same time step then dividing the difference by the minimum value and multiply it by 100 to get the random error percentage as shown in the following equation:

$$E = \frac{Max - Min}{Min} \times 100 \quad (4.8)$$

The difference between maximum and minimum values are reported in Table 13 along with random error percentage for each case.

Table 13: Random error calculation.

	Fuel (GOX), lpm	Time (s)	Min	Max	Unit	Error %
Pressure	Date Sone (110)	29.5	1.52	1.87	Bar	23
	Paraffin Wax (80)	24.5	1.78	1.95	Bar	10
Thrust	Date Sone (110)	29	17.0	28.0	N	65
	Paraffin Wax (80)	16	45	56	N	24

Chapter 5: Conclusion

This study investigated the performance of biomass solid waste as an HRM propellant. The variation of performance among the proposed fuels was obvious, especially comparing the biomass propellant to the reference PW-based propellant. Combustion chamber pressure, thrust, combustion chamber temperature profile, and flame length generated suggested that the reference propellant performed much better than biomass solid propellants. Biomass propellants showed similar propulsion performance. However, a combustion characteristic study has been conducted for biomass fuel and showed an advantage for Date Stone grains in terms of volatile matter and fixed carbon content compared to Jojoba. Based on that, Jojoba propellant requires a higher O/F ratio for more complete combustion, as proven practically in Section 4.2.

In terms of stability, the Date Stone propellant showed more stable pressure and thrust profiles while increasing the oxidizer volume flow rate. With a higher oxidizer volume flow rate, the gap in the combustion chamber pressure profile between Date Stone and Jojoba tends to be larger, which means Date Stone pressure increases at a higher rate with flow rate compared to Jojoba propellant. However, a similar situation with a thrust profile but with clear consistency.

5.1 Propellant Feasibility

This study investigated the performance of two biomass solid fuels along with a PW-based fuel as a reference for comparison. Considering all measured propulsion parameters, PW-based propellant showed clear supremacy and recorded higher combustion chamber pressure, thrust, and flame length profiles for all runs under all oxidizer volume flow rates. Therefore, the proposed solid biomass propellant under

current measurement conditions can't be considered to replace hydrocarbon fuels such as Paraffin Wax. Although the propulsion performance of biomass solids could not challenge typical fuel, there are many applications where proposed biomass fuels can be a good fit, such as furnaces, considering the measured combustion characteristics.

5.2 Recommendations for Future Work

Biomass fuel showed decent combustion characteristics in TGA tests and experimental firing runs. However, in comparison with typical hydrocarbon fuels such as Paraffin-Wax based, a lower performance was detected for pure biomass grains. Usually, researchers tend to increase propellant performance by adding metallic additives or playing with the port size, shape, and orientation. Metallic additives to increase the burning efficiency are expected to enhance the performance of proposed biomass propellants. Moreover, the ignition system used in this study wasn't the best ignition system possible. Therefore, a more efficient ignition system would result in a better burning start. Finally, many modifications can be implemented to improve biomass testing as fuel in HRM and this study paves the road for more research and experimental studies of biomass fuel in hybrid or solid rocket engine systems.

References

- [1] L. T. DeLuca, “Highlights of solid rocket propulsion history,” in *Chemical Rocket Propulsion*, Springer, 2017.
- [2] A. Davenas, “Development of modern solid propellants,” *J. Propuls. power*, vol. 19, no. 6, pp. 1108–1128, 2003.
- [3] M. Barrere, A. Jaumotte, B. Fraeijs de Veubeke, and J. Vandekerckhove, “Rocket propulsion”, vol. 47, pp. 10, 1960.
- [4] D. P. Mishra ”*Fundamentals of rocket propulsion*” CRC Press. 2017.
- [5] A. Davenas ”*Solid rocket propulsion technology*”, Newnes. 2012.
- [6] M. L. Corradini, C. Zhu, L. S. Fan, and R. H. Jean, ”*Rocket Propulsion Elements*”, Seventh edition, 2016.
- [7] S. D. Heister, W. E. Anderson, T. L. Pourpoint, and R. J. Cassady ”*Rocket propulsion*”, Cambridge University Press, 2019.
- [8] P. D. I. Milano, P. L. T. D. E. Luca, and P. S. Ricci, “Ballistics of Innovative Solid Fuel Formulations for Hybrid Rocket Engines”, 2012.
- [9] R. Royce, ”*The jet engine*”, Fifth edition. 1986.
- [10] D. Altman and A. Holzman, “Overview and History of Hybrid Rocket Propulsion, Fundamentals of Hybrid Rocket Combustion and Propulsion, Vol. 218, Edited by MJ Chiaverini, and KK Kuo,” *Prog. Astronaut. Aeronaut. AIAA, Reston, VA*, 2007.
- [11] L. T. DeLuca, “Energetic Problems in Aerospace Propulsion, Notes for Students.” Premani, Pantigliate-Milano, Italy, Revised and Extended Preliminary Edition, 2009.
- [12] K. P. Cardoso, L. F. A. Ferrão, E. Y. Kawachi, T. B. Araújo, R. F. Nunes, and M. Y. Nagamachi, “Preparation of paraffin-based solid combustible for hybrid propulsion rocket motor,” *J. Propuls. Power*, vol. 33, no. 2, pp. 448–455, 2017.
- [13] D. Altman, “Rocket Motors, Hybrid,” *Encycl. Phys. Sci. Technol.*, pp. 303–321, 2003.
- [14] M. A. Karabeyoglu, D. Altman, and B. J. Cantwell, “Combustion of liquefying hybrid propellants: Part 1, general theory,” *J. Propuls. Power*, vol. 18, no. 3, pp. 610–620, 2002.
- [15] B. Cantwell, A. Karabeyoglu, and D. Altman, “Recent advances in hybrid propulsion,” *Int. J. Energ. Mater. Chem. Propuls*, vol. 9, no. 4, 2010.

- [16] L. T. DeLuca *et al.*, “Characterization of HTPB-based solid fuel formulations: Performance, mechanical properties, and pollution,” *Acta Astronaut*, vol. 92, no. 2, pp. 150–162, 2013.
- [17] U. Vellaisamy and S. Biswas, “Effect of metal additives on neutralization and characteristics of AP/HTPB solid propellants,” *Combust. Flame*, vol. 221, pp. 326–33, 2020.
- [18] B. P. Mason and C. M. Roland, “Solid propellants,” *Rubber Chem. Technol*, vol. 92, no. 1, pp. 1–24, 2020.
- [19] S. Chaturvedi and P. N. Dave, “Solid propellants: AP/HTPB composite propellants,” *Arab. J. Chem*, vol. 12, no. 8, pp. 2061–2068, 2019.
- [20] A. E.-S. Makled, “Hybrid Rocket Motor: Propellant Selection and Fuel Grain Design,” in *The International Conference on Chemical and Environmental Engineering*, 2016, vol. 8, no. 8th International Conference on Chemical & Environmental Engineering, pp. 261–281.
- [21] R. Aggarwal, I. Patel, and P. B. Sharma, “Green propellant: A study,” *Int. J. Latest Trends Eng. Technol*, vol. 6, no. 1, pp. 83–87, 2015.
- [22] I. E. H. Belal, “Evaluating fungi-degraded date pits as a feed ingredient for Nile tilapia *Oreochromis niloticus* L.,” *Aquac. Nutr*, vol. 14, no. 5, pp. 445–452, 2008.
- [23] H. H. Sait, A. Hussain, A. Adam, and F. Nasir, “Bioresource Technology Pyrolysis and combustion kinetics of date palm biomass using thermogravimetric analysis,” *Bioresour. Technol*, vol. 118, pp. 382–389, 2012.
- [24] E. Elnajjar, S. Al-zuhair, S. Hasan, S. Almardeai, S. A. B. Al Omari, and A. Hilal-alnaqbi, “Morphology characterization and chemical composition of United Arab Emirates date seeds and their potential for energy production,” *Energy*, vol. 213, p. 118810, 2020, doi: 10.1016/j.energy.2020.118810.
- [25] Y. Elmay, M. Jeguirim, S. Dorge, G. Trouvé, and R. Said, “Evaluation of date palm residues combustion in fixed bed laboratory reactor : A comparison with sawdust behaviour,” *Renew. Energy*, vol. 62, pp. 209–215, 2014.
- [26] U. Al-Omari. Emirates, “Evaluation of the biomass ‘ date stones ’ as a fuel in furnaces : A comparison with coal combustion ☆,” *Int. Commun. Heat Mass Transf*, vol. 36, no. 9, pp. 956–961, 2009.
- [27] J. J. Al Asfar, A. Alshwawra, A. Sakhrieh, and A. Mohammad, “Environmental Effects Combustion characteristics of solid waste biomass , oil shale , and coal,” *Energy Sources, Part A Recover. Util. Environ. Eff*, pp. 1–8, 2017.

- [28] B. Al-Omari, "Experimental investigation on combustion and heat transfer characteristics in a furnace fueled with unconventional biomass fuels (date stones and palm stalks)", vol. 47, pp. 778–790, 2006.
- [29] R. Briones, L. Serrano, R. Ben, and J. Labidi, "Polyol production by chemical modification of date seeds", vol. 34, pp. 1035–1040, 2011.
- [30] M. E. Babiker, A. R. A. Aziz, M. Heikal, S. Yusup, and M. Abakar, "Pyrolysis Characteristics of Phoenix Dactylifera Date Palm Seeds Using Thermo-Gravimetric Analysis (TGA)", vol. 4, no. 5, pp. 521–524, 2013.
- [31] M. I. Al-widyan and M. A. Al-muhtaseb, "Experimental investigation of jojoba as a renewable energy source," *Energy Convers. Manag.*, vol. 51, no. 8, pp. 1702–1707, 2013.
- [32] J. Wisniak, *The chemistry and technology of jojoba oil*. The American Oil Chemists Society, 1987.
- [33] L. Canoira, R. Alcantara, M. J. García-Martínez, and J. Carrasco, "Biodiesel from Jojoba oil-wax: Transesterification with methanol and properties as a fuel," *Biomass and Bioenergy*, vol. 30, no. 1, pp. 76–81, 2006.
- [34] M. Y. E. Selim, M. S. Radwan, and S. M. S. Elfeky, "Combustion of jojoba methyl ester in an indirect injection diesel engine", vol. 28, pp. 1401–1420, 2003.
- [35] M. Y. E. Selim, M. S. Radwan, and H. E. Saleh, "Improving the performance of dual fuel engines running on natural gas/LPG by using pilot fuel derived from jojoba seeds," *Renew. energy*, vol. 33, no. 6, pp. 1173–1185, 2008.
- [36] M. Y. E. Selim, M. S. Radwan, and H. E. Saleh, "On the use of jojoba methyl ester as pilot fuel for dual fuel engine running on gaseous fuels," *SAE Int.*, pp. 24–121, 2007.
- [37] M. S. Radwan, S. K. Dandoush, M. Y. E. Selim, and A. M. A. Kader, "*Ignition delay period of jojoba diesel engine fuel*", Society of Automotive Engineers, 1997.
- [38] S. N. Shah, B. K. Sharma, and B. R. Moser, "Preparation of biofuel using acetylation of jojoba fatty alcohols and assessment as a blend component in ultralow sulfur diesel fuel," *Energy & fuels*, vol. 24, no. 5, pp. 3189–3194, 2010.
- [39] M. O. Hamdan and M. Y. E. Selim, "Performance of CI engine operating with hydrogen supplement co-combustion with jojoba methyl ester," *Int. J. Hydrogen Energy*, vol. 41, no. 24, pp. 10255–10264, 2016.
- [40] A. I. EL-Seesy, Z. He, H. Hassan, and D. Balasubramanian, "Improvement of combustion and emission characteristics of a diesel engine working with diesel/jojoba oil blends and butanol additive," *Fuel*, vol. 279, pp. 118433, 2020, <https://doi.org/10.1016/j.fuel.2020.118433>.

- [41] M. Y. E. Selim and S. Radwan, "International Journal of Sustainable Utilization of extracted jojoba fruit as a fuel", pp. 37–41, 2014.
- [42] C. Paravan, M. Manzoni, G. Rambaldi, and L. T. De Luca, "Analysis of quasi-steady and transient burning of hybrid fuels in a laboratory-scale burner by an optical technique," *Int. J. Energ. Mater. Chem. Propuls*, vol. 12, no. 5, pp. 385-410, 2013.
- [43] M. A. Karabeyoglu and B. J. Cantwell, "Combustion of liquefying hybrid propellants: Part 2, stability of liquid films," *J. Propuls. Power*, vol. 18, no. 3, pp. 621–630, 2002.
- [44] Y. Pal and V. Ravikumar, "ScienceDirect Mechanical Characterization of Paraffin-Based Hybrid Rocket Fuels," *Mater. Today Proc*, vol. 16, pp. 939–948, 2019.
- [45] S. Venugopal, K. K. Rajesh, and V. Ramanujachari, "Hybrid Rocket Technology", vol. 61, no. 3, pp. 193–200, 2011.
- [46] M. Boiocchi, F. Maggi, C. Paravan, and L. Galfetti, "Paraffin-based fuels and energetic additives for hybrid rocket propulsion," in *51st AIAA/SAE/ASEE Joint Propulsion Conference*, 2015.
- [47] S. Kim, H. Moon, J. Kim, and J. Cho, "Evaluation of paraffin–polyethylene blends as novel solid fuel for hybrid rockets," *J. Propuls. Power*, vol. 31, no. 6, pp. 1750–1760, 2015.
- [48] Y. Pal, K. H. Kumar, and Y.-H. Li, "Ballistic and mechanical characteristics of paraffin-based solid fuels," *CEAS Sp. J.*, vol. 11, no. 3, pp. 317–327, 2019.
- [49] Y. Pal and V. R. Kumar, "Thermochemical Acta Thermal decomposition study of paraffin based hybrid rocket fuel containing Aluminum and Boron additives". vol. 655, pp. 63–75, 2017.
- [50] Y. J. Kim, C. H. Sohn, M. Hong, and S. Y. Lee, "An analysis of fuel–oxidizer mixing and combustion induced by swirl coaxial jet injector with a model of gas–gas injection," *Aerosp. Sci. Technol*, vol. 37, pp. 37–47, 2014.
- [51] L. Merotto, M. Boiocchi, F. Maggi, L. T. De Luca, P. Doctoral, and P. Doctoral, "Ballistic and rheological characterization of paraffin-based fuels for hybrid rocket propulsion", pp. 1–17, 2011.
- [52] L. Galfetti, L. De Luca, C. Paravan, L. Merotto, and M. Boiocchi, "Regression Rate and CCPs Measurement of Metallized Solid Fuels," in *8th International Symposium on Special Topics in Chemical Propulsion (8-ISICP)*, 2009, pp. 1–12.
- [53] M. J. Chiaverini, "Review of Solid-Fuel Regression Rate Behavior in Classical and Nonclassical Hybrid Rocket Motors," *Fundam. hybrid Rocket Combust. Propuls*, pp. 49–92, 2007.

- [54] R. A. Nasser *et al.*, “Chemical analysis of different parts of date palm (Phoenix dactylifera L.) using ultimate, proximate and thermo-gravimetric techniques for energy production,” *Energies*, vol. 9, no. 5, p. 374, 2016, <https://doi.org/10.3390/en9050374>.
- [55] T. Sakurai, S. Yuasa, H. Ando, K. Kitagawa, and T. Shimada, “Performance and regression rate characteristics of 5-kN swirling-oxidizer-flow-type hybrid rocket engine,” *J. Propuls. Power*, vol. 33, no. 4, pp. 891–901, 2017.
- [56] Y. Wang, S. Hu, X. Liu, and L. Liu, “Regression rate modeling of HTPB/paraffin fuels in hybrid rocket motor,” *Aerosp. Sci. Technol*, vol. 121, pp. 107324, 2022, <https://doi.org/10.1016/j.ast.2021.107324>.

The logo for the United Arab Emirates University (UAEU) is displayed in a red rectangular box. It consists of the letters "UAEU" in a white, bold, sans-serif font.

جامعة الإمارات العربية المتحدة
United Arab Emirates University



UAE UNIVERSITY MASTER THESIS NO. 2022:50

This research investigates experimentally the performance of two solid biomass wastes as propellants for Hybrid Rocket Motor based on the combustion and propulsion parameters. The main objective of this study is to examine the performance of the proposed fuels in comparison with the typical hydrocarbon fuel, Paraffin Wax.

www.uaeu.ac.ae

Saleh Mohammed Musaed Badi received his Master of Science in Mechanical Engineering from the Department of Mechanical and Aerospace Engineering, College of Engineering at UAE University, UAE. He received his BSc in Mechanical Engineering from the College of Engineering, University of Sharjah, UAE.